48/3-31-92 JS (2)

PREPARED FOR THE U.S. DEPARTMENT OF ENERGY,
UNDER CONTRACT DE-AC02-76-CHO-3073

PPPL-2831
UC-427

PPPL-2831

ATOMIC PHYSICS EFFECTS ON DISSIPATIVE TOROIDAL DRIFT WAVE STABILITY

BY

M.A. BEER AND T.S. HAHM

February 1992

PPPL PRINCETON PLASMA PHYSICS LABORATORY

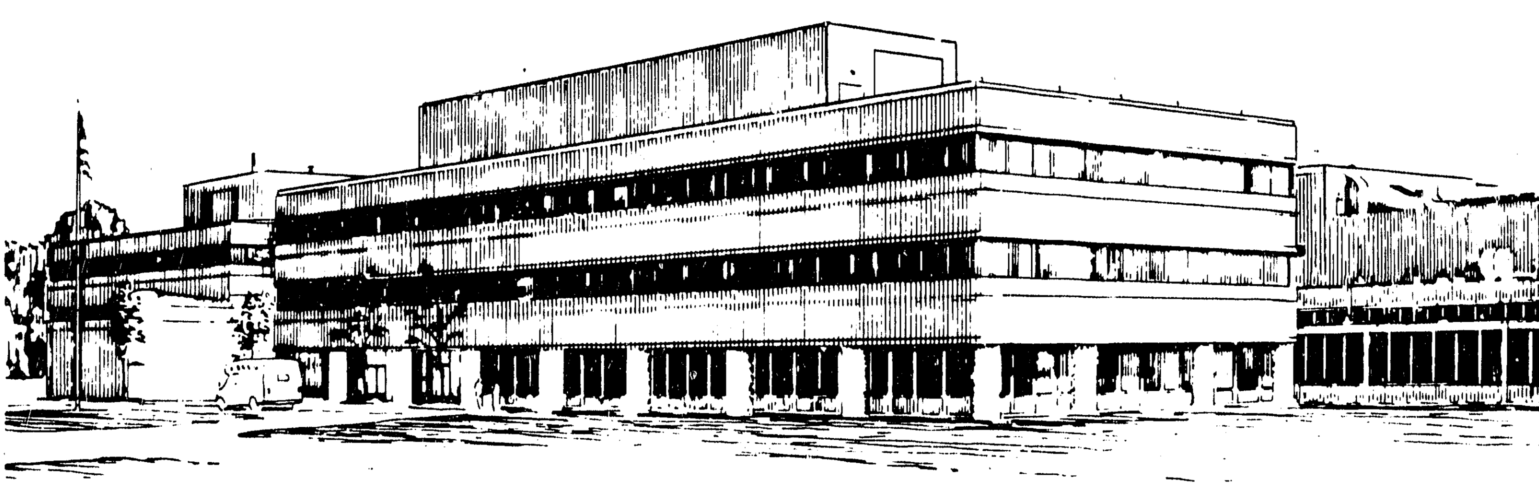

PPPL--2831

DE92 010007

Atomic Physics Effects on Dissipative Toroidal Drift Wave Stability

M. A. Beer and T. S. Hahm
Princeton Plasma Physics Laboratory, Princeton University
Princeton, New Jersey 08543

Abstract

The effects of atomic physics processes such as ionization, charge exchange, and radiation on the linear stability of dissipative drift waves are investigated in toroidal geometry both numerically and analytically. For typical TFTR and TEXT edge parameters, overall linear stability is determined by the competition between the destabilizing influence of ionization and the stabilizing effect due to the electron temperature gradient. An analytical expression for the linear marginal stability condition, η_e^{crit}, is derived. The instability is most likely to occur at the extreme edge of tokamaks with a significant ionization source and a steep electron density gradient.

PACS numbers: 52.35.Kt, 52.35.Qz, 52.25.Gj, 52.55.Fa

I Introduction

Tokamak edge plasmas are characterized by large density and potential fluctuations and large particle diffusivity, which typically increases toward the edge as a function of minor radius.[1-3] Most previous drift wave turbulence models have not been successful in explaining the radial profile of the diffusivity and the large fluctuation levels.[4] Another widely studied edge turbulence candidate is resistivity gradient driven turbulence[5] which evolves from the rippling instability[6] in the linear regime. Although this model predicts larger fluctuation levels and radially increasing particle diffusivities, it suffers from the explicit dependence on the edge current density, which has been called into question by a number of current ramp experiments.[7,8] However, the radial gradient of the toroidal electric field which develops during the ramp could drive some residual instability. Including realistic effects such as the impurity dynamics[9,10] and radiation[11] tends to make the theoretical predictions closer to experimental observations.

Recently, drift wave turbulence has been reconsidered including atomic physics effects with a hope that the aforementioned problems could be remedied. Most of these efforts have been performed in a simplified geometry, with a focus on the nonlinear regime.[12,13]

In this paper, we consider the effects of atomic physics on the linear stability of dissipative drift waves in toroidal geometry. It has been shown that in toroidal geometry, the coupling of adjacent poloidal harmonics renders magnetic shear induced damping ineffective.[14] Therefore, the instability with toroidal mode structure is more likely to be excited than one with Pearlstein-Berk mode structure.

The principal conclusions of this paper include:

i. For typical TFTR and TEXT edge parameters, atomic physics effects are only important for long wavelength modes. In order of relative importance: ionization is destabilizing, charge-exchange is stabilizing, and radiation effects are smaller.

ii. It is shown that *nonlocal* analysis is necessary to properly determine stablility.

iii. For typical parameters, the toroidal mode structure[14] is maintained in the presence of atomic physics effects. The electron dynamics are nearly adiabatic (Boltzmann-like), rather than hydrodynamic, over most of the width of the eigenmode, although the deviation from adiabaticity is crucial and non-negligible.

iv. Various asymptotic regimes in parameter space are identified and fluctuation characteristics are discussed for each regime. Relations to previous works are elucidated.

The organization of the rest of this paper is as follows. In Sec. II, we present the basic model and obtain the dispersion relation in the local limit. The basic trends atomics physics effects have on stability are indicated by local analysis. We turn to the nonlocal analysis in Sec. III, where we derive the eigenmode equation using the ballooning transformation, and solve it both numerically and analytically. Conclusions and discussion of these results are presented in Sec. IV.

II Theoretical Model and Local Analysis

The basic model for dissipative drift waves can be derived from the Braginskii fluid equations.[15] To properly include atomic physics effects, we take moments of the Boltzmann equation:

$$\frac{\partial f}{\partial t} + \mathbf{v} \cdot \nabla_x f + \frac{q}{m}\left(\mathbf{E} + \frac{\mathbf{v} \times \mathbf{B}}{c}\right) \cdot \nabla_v f = \frac{\delta f}{\delta t}.$$

obtaining, for the zeroth, first, and second velocity moments:

$$\begin{aligned}
\frac{\partial n}{\partial t} + \nabla \cdot (n\mathbf{u}) &= \int_{-\infty}^{\infty} d\mathbf{v} \frac{\delta f}{\delta t}, & (1)\\
nm\frac{d\mathbf{u}}{dt} &= -\nabla p + qn\left(\mathbf{E} + \frac{\mathbf{u}\times\mathbf{B}}{c}\right) + m\int_{-\infty}^{\infty} d\mathbf{v}\frac{\delta f}{\delta t}(\mathbf{v}-\mathbf{u}), & (2)\\
\frac{3}{2}n\frac{dT}{dt} &= -p\nabla\cdot\mathbf{u} - \nabla\cdot\mathbf{q} + \frac{m}{2}\int_{-\infty}^{\infty} d\mathbf{v}\frac{\delta f}{\delta t}(\mathbf{v}-\mathbf{u})^2 - T\int_{-\infty}^{\infty} d\mathbf{v}\frac{\delta f}{\delta t}. & (3)
\end{aligned}$$

Atomic physics processes and collisions enter these moment equations through the velocity space integrals of

$$\frac{\delta f}{\delta t} = \left(\frac{\delta f}{\delta t}\right)_{coll} + \left(\frac{\delta f}{\delta t}\right)_{ion} + \left(\frac{\delta f}{\delta t}\right)_{cx} + \left(\frac{\delta f}{\delta t}\right)_{rad}.$$

Therefore, the usual cold ion Braginskii equations are modified in the following way:

$$\begin{aligned}
\frac{\partial n_e}{\partial t} + \nabla \cdot (n_e\mathbf{v}_e) &= S_e, & (4)\\
m_e n_e\frac{d\mathbf{v}_e}{dt} &= -\nabla p_e - en_e(\mathbf{E} + \frac{\mathbf{v}_e\times\mathbf{B}}{c}) + \mathbf{R}_{ei} + m_e S_e(\mathbf{v}_N - \mathbf{v}_e), & (5)\\
\frac{3}{2}n_e\frac{dT_e}{dt} &= -p_e\nabla\cdot\mathbf{v}_e - \nabla\cdot\mathbf{q}_e + Q_{ei} - P_{rad} - T_e S_e + \frac{m_e}{2}S_e(\mathbf{v}_N - \mathbf{v}_e)^2, & (6)\\
\frac{\partial n_i}{\partial t} + \nabla \cdot (n_e\mathbf{v}_i) &= S_i, & (7)\\
m_i n_i\frac{d\mathbf{v}_i}{dt} &= en_i(\mathbf{E} + \frac{\mathbf{v}_i\times\mathbf{B}}{c}) - \mathbf{R}_{ei} + m_i D_i(\mathbf{v}_N - \mathbf{v}_i) + m_i S_i(\mathbf{v}_N - \mathbf{v}_i). & (8)
\end{aligned}$$

The atomic physics effects are contained in:

$$\begin{aligned}
S_e = S_i &= n_e n_N \langle\sigma v\rangle_{ion}\\
D_i &= n_i n_N \langle\sigma v\rangle_{cx}\\
P_{rad} &= n_e n_z L_z(T_e)
\end{aligned}$$

for ionization, charge exchange, and radiation, respectively. Physically ionization is a source in the electron and ion continuity equations, charge exchange causes drag on the ion parallel velocity, and radiation cools the electrons. Note that while ionization does not affect the fluid momentum ($n\mathbf{v}$) or energy (nT), it appears as a drag in the velocity equation, and also enters the temperature equation.

For electrostatic perturbations with $\omega \ll \Omega_i$, the perpendicular dynamics are governed by:

$$\mathbf{v}_{\perp e} = \mathbf{v}_{E\times B} + \mathbf{v}_{de} \qquad \mathbf{v}_{E\times B} = -\frac{c}{B^2}\nabla_\perp\Phi\times\mathbf{B}$$

$$\mathbf{v}_{\perp i} = \mathbf{v}_{E\times B} + \mathbf{v}_{pi} \qquad \mathbf{v}_{de} = -\frac{c}{eB^2 n_e}\mathbf{B}\times\nabla_\perp p_e$$

$$\mathbf{v}_{pi} = -\frac{c}{B\Omega_i}\frac{\partial}{\partial t}\nabla_\perp\Phi.$$

Here we have used $m_i \gg m_e$ and assumed $T_i \ll T_e$ for simplicity.

In a toroidal system, the divergence of the $\mathbf{E}\times\mathbf{B}$ drift in the ion continuity equation does not vanish, and leads to coupling between different poloidal harmonics. For a large aspect ratio torus with concentric circular flux surfaces, we have $\nabla_\perp\cdot\mathbf{v}_{E\times B} = -2i\omega_{de}\left(\cos\theta - \frac{i}{k_\theta}\sin\theta\frac{\partial}{\partial r}\right)\frac{e\Phi}{T}$, where $\omega_{de} = \frac{k_\theta \rho_s c_s}{R}$.

We linearize Eqs. (4)-(8) with $n_e = n_0 + n_{e1}$, $n_i = n_0 + n_{i1}$, $p_e = p_0 + p_{e1}$, $T_e = T_0 + T_{e1}$, $v_\parallel = v_{\parallel 1}$, assuming there is no mean flow ($v_{\parallel 0} = 0$). The neutral velocity is assumed to be stationary compared to the perturbed ion and electron velocities. We also assume that the wavelengths of the fluctuations are much shorter than the equilibrium gradient scale lengths ($L_n, L_T, \ldots$) but comparable to the ion gyroradius at the electron temperature, $\rho_s = \frac{c_s}{\Omega_i}$. Defining the following dimensionless field quantities,

$$\tilde{n}_e = \frac{n_{e1}}{n_0},\ \tilde{n}_i = \frac{n_{i1}}{n_0},\ \tilde{v}_i = \frac{v_{\parallel i}}{c_s},\ \tilde{v}_e = \frac{v_{\parallel e}}{c_s},\ \tilde{T} = \frac{T_{e1}}{T_0},\ \tilde{\Phi} = \frac{e\Phi}{T_0}$$

and the following atomic process rates,

$$\begin{aligned}\beta_n &= \frac{\partial S_e}{\partial n_e} = n_N\langle\sigma v\rangle_{ion} \\ \beta_T &= \frac{T_0}{n_0}\frac{\partial S_e}{\partial T_e} = n_N T_0\frac{\partial\langle\sigma v\rangle_{ion}}{\partial T_e}\end{aligned}$$

$$\begin{aligned}
\gamma_v &= \frac{D_i}{n_0} = n_N \langle \sigma v \rangle_{cx} \\
\gamma_n &= \frac{2}{3}\frac{1}{T_0}\frac{\partial P_{rad}}{\partial n_e} = \frac{2}{3}\frac{n_z}{T_0} L_z \\
\gamma_T &= \frac{2}{3}\frac{1}{n_0}\frac{\partial P_{rad}}{\partial T_e} = \frac{2}{3} n_z \frac{\partial L_z}{\partial T_e}
\end{aligned}$$

we have,

$$\tilde{n}_e = \frac{\omega_*}{\omega}\tilde{\Phi} + \frac{k_{\|}c_s}{\omega}\tilde{v}_e + i\frac{\beta_n}{\omega}\tilde{n}_e + i\frac{\beta_T}{\omega}\tilde{T} \tag{9}$$

$$0.51\,\nu_{ei}(\tilde{v}_i - \tilde{v}_e) = i\frac{k_{\|}v_{te}^2}{c_s}(\tilde{n}_e - \tilde{\Phi} + 1.71\tilde{T}) + \beta_n \tilde{v}_e + i\omega\tilde{v}_e \tag{10}$$

$$\begin{aligned}
\tilde{T} = {} & \eta_e \frac{\omega_*}{\omega}\tilde{\Phi} + \frac{2}{3}\frac{k_{\|}c_s}{\omega}\tilde{v}_e - i\frac{2}{3}3.16\frac{k_{\|}^2 v_{te}^2}{\omega\nu_{ei}}\tilde{T} - \frac{2}{3}0.71\frac{k_{\|}c_s}{\omega}(\tilde{v}_i - \tilde{v}_e) \\
& - i\frac{\gamma_n}{\omega}\tilde{n}_e - i\frac{\gamma_T}{\omega}\tilde{T} - i\frac{2}{3}\left(\frac{\beta_n}{\omega}\tilde{n}_e + \frac{\beta_n}{\omega}\tilde{T} + \frac{\beta_T}{\omega}\tilde{T}\right)
\end{aligned} \tag{11}$$

$$\begin{aligned}
\tilde{n}_i = {} & \left(\frac{\omega_*}{\omega} - 2\frac{\omega_{de}}{\omega}(\cos\theta - \frac{i}{k_\theta}\sin\theta\frac{\partial}{\partial r}) + \rho_s^2(\frac{\partial^2}{\partial r^2} - k_\theta^2)\right)\tilde{\Phi} + \frac{k_{\|}c_s}{\omega}\tilde{v}_i \\
& + i\frac{\beta_n}{\omega}\tilde{n}_e + i\frac{\beta_T}{\omega}\tilde{T}
\end{aligned} \tag{12}$$

$$\tilde{v}_i = \frac{k_{\|}c_s}{\omega}\left(\tilde{n}_e + \tilde{T}\right) - i\frac{\gamma_v}{\omega}\tilde{v}_i - i\frac{\beta_n}{\omega}\tilde{v}_i \tag{13}$$

where the numerical factors come from the Braginskii coefficients ($\eta_{\|} = 0.51\frac{m_e\nu_{ei}}{ne^2}$, $\kappa_{\|} = 3.16\frac{nT}{m_e\nu_{ei}}$, $\alpha = 1.71$) and $\eta_e = \frac{L_n}{L_T}$, $\omega_* = \frac{k_\theta\rho_s c_s}{L_n}$. We note that density and temperature fluctuations affect the ionization source (β_n, β_T), and the radiated power (γ_n, γ_T).

Before presenting the solution of the eigenmode equation (in Sec. III), which is necessary to accurately determine the stability of this system, we begin by examining the local dispersion relation. For the purposes of this discussion, we treat the ω_{de} term as a constant, evaluated at $\theta = 0$ (bad curvature side), and treat $-\frac{\partial^2}{\partial r^2} - k_\theta^2$ as a constant, $k_\perp^2$. In this local limit,

$$\tilde{n}_i = \left(\frac{\omega_*}{\omega} - 2\frac{\omega_{de}}{\omega} - k_\perp^2\rho_s^2\right)\tilde{\Phi} + \frac{k_{\|}c_s}{\omega}\tilde{v}_i + i\frac{\beta_n}{\omega}\tilde{n}_e + i\frac{\beta_T}{\omega}\tilde{T}. \tag{14}$$

Using quasineutrality and Eqs. (9)-(11) and (13), we can obtain the local dispersion relation.

Two dimensionless parameters play crucial roles in characterizing the properties of the fluctuations: $\frac{k_\parallel^2 v_{te}^2}{\omega \nu_{ei}}$ and $\frac{k_\parallel^2 c_s^2}{\omega^2}$. The first, $\frac{k_\parallel^2 v_{te}^2}{\nu_{ei}}$ comes from the $\kappa_\parallel \nabla_\parallel^2 T_e$ term in $\nabla \cdot \mathbf{q}_e$, and measures electron thermal conduction along $\mathbf{B}$. Thus the parameter $\frac{k_\parallel^2 v_{te}^2}{\omega \nu_{ei}}$ compares the parallel electron thermal conduction rate to the mode frequency. The second, $\frac{k_\parallel c_s}{\omega}$ is the ratio of the sound wave propagation rate along $\mathbf{B}$ to the mode frequency. When $\frac{k_\parallel^2 v_{te}^2}{\omega \nu_{ei}} \gg 1$, electron thermal conduction is strong enough to smooth temperature fluctuations along $\mathbf{B}$, so $\tilde{T}_e \to 0$. This is known as the adiabatic limit, and electrons have a Boltzmann-like distribution. When $\frac{k_\parallel^2 c_s^2}{\omega^2} \gg 1$, sound waves smooth pressure perturbations along $\mathbf{B}$, so $\tilde{p}_e \to 0$. This will be called the pressure balance limit in this paper.

As will be shown in Sec. III using the nonlocal mode structure, the adiabatic regime is relevant for typical tokamak edge parameters. We discuss several other limits to relate this work to previous studies.

i). In the adiabatic regime, $\frac{k_\parallel^2 v_{te}^2}{\omega \nu_{ei}} \gg 1$, $\frac{k_\parallel^2 c_s^2}{\omega^2}$:

$$\tilde{n}_e \simeq \tilde{\Phi}, \qquad \tilde{T} \simeq 0, \qquad \tilde{v}_i \simeq \frac{k_\parallel c_s}{\omega + i\gamma_v + i\beta_n} \tilde{\Phi}. \tag{15}$$

Quasi-neutrality gives the following dispersion relation to the leading order in $\frac{\omega \nu_{ei}}{k_\parallel^2 v_{te}^2}$:

$$\omega^2(1+b) - \omega\left(\omega_* - 2\omega_{de} + i\beta_n - i(1+b)(\gamma_v + \beta_n)\right) - k_\parallel^2 c_s^2 - i(\gamma_v + \beta_n)(\omega_* - 2\omega_{de} + i\beta_n) = 0, \tag{16}$$

where $b = k_\perp^2 \rho_s^2$. When $k_\parallel c_s$, γ_v, $\beta_n \ll \omega$, the electron root further reduces to:

$$\omega_0 \simeq \frac{\omega_* - 2\omega_{de} + i\beta_n}{1+b} + \frac{k_\parallel^2 c_s^2}{(\omega_* - 2\omega_{de})^2}\left[\omega_* - 2\omega_{de} - i\beta_n - i(\beta_n + \gamma_v)(1+b)\right]. \tag{17}$$

In the local approximation, the destabilizing effect of ionization (β_n) comes from the inverse dissipation in the ion continuity equation. The stabilizing influence due to the ionization and charge-exchange drag on the parallel ion velocity is smaller roughly by a factor of $\frac{k_\parallel^2 c_s^2}{\omega^2}$. When spatially dependent $k_\parallel$ is actually taken into account, a nonlocal analysis in Sec. III shows that the overall effect of ionization is destabilizing. Therefore, the ionization term in the ion velocity equation, which is often neglected in the previous studies, seems to be important only when $\frac{k_\parallel^2 c_s^2}{\omega^2} \gtrsim 1$. We also note that the real frequency is shifted below ω_* by ω_{de} and finite Larmor radius effects. Because $\tilde{T}$ is small in this regime, radiation effects are subdominant.

Collisional effects appear as a first order ($\sim \frac{\omega\nu_{ei}}{k_\parallel^2 v_{te}^2}$) correction to ω_0 in Eq. (16);

$$\omega \simeq \omega_0 + i\frac{0.812}{(1+b)^2}\frac{\omega_*^2\nu_{ei}}{k_\parallel^2 v_{te}^2}\left[1.77(1-\frac{\omega_0}{\omega_*}) - \eta_e\right]. \tag{18}$$

Collisional effects are destabilizing when the down-shift of ω overcomes the stabilizing effects of η_e, i.e., $\eta_e < 1.77(1-\frac{\omega}{\omega_*})$. When the spatial dependence of $k_\parallel$ is treated nonlocally in the next section, this scaling with ν_{ei} changes to $\nu_{ei}^{\frac{1}{2}}$, increasing the relative importance of collisional effects. Radiation effects also enter at this order in $\frac{\omega\nu_{ei}}{k_\parallel^2 v_{te}^2}$, but only shift the real frequency, and do not affect stability directly.

ii). In the hydrodynamic regime, $\frac{k_\parallel^2 v_{te}^2}{\omega\nu_{ei}}, \frac{k_\parallel^2 c_s^2}{\omega^2} \ll 1$:

$$\tilde{n}_e \simeq \frac{\omega_*}{\omega}\tilde{\Phi}, \qquad \tilde{T}_e \simeq \eta_e\frac{\omega_*}{\omega}\tilde{\Phi}.$$

Here the dynamics along $\mathbf{B}$ is insignificant, and the electron density and temperature are mainly $\mathbf{E}\times\mathbf{B}$ convected. Note that if $\eta_e \gg 1$, we recover the limit considered by Ware, *et al.*[12] where $\omega \sim \eta\omega_* = \omega_{*T}$ and $\tilde{T} \sim \tilde{\Phi} \gg \tilde{n}_e$ In this limit, radiation effects could be significant.

iii). In the pressure balance regime, $\frac{k_{\|}^2 c_s^2}{\omega^2} \gg 1, \frac{k_{\|}^2 v_{te}^2}{\omega \nu_{ei}}$:

$$\tilde{n}_e \simeq -\tilde{T} \simeq \left[\frac{\frac{\omega_*}{\omega}(\frac{2}{3} - \eta_e) + i\, 1.82 \frac{k_{\|}^2 v_{te}^2}{\omega \nu_{ei}}}{\frac{5}{3} + i\, 5.51 \frac{k_{\|}^2 v_{te}^2}{\omega \nu_{ei}}} \right] \tilde{\Phi}$$

This limit is similar to the one investigated by Drake, *et al.*[16] for the case $\tilde{\mathrm{J}} \simeq 0$. In contrast to the near adiabatic regime, the pressure balance regime permits large electron temperature fluctuations, and consequently, radiation could become an important destabilizing effect.

III Nonlocal Analysis

We derive the linear eigenmode equation using the ballooning formalism.[17–19] This procedure reduces the two dimensional problem in (r, θ) to a one dimensional eigenmode equation in the ballooning coordinate (η), which can be regarded as the coordinate along the field lines. The simplifying assumption is that for large mode numbers m, different poloidal harmonics have nearly identical structures centered at each rational surface.

Using quasineutrality, Eqs. (12) and (13) become:

$$\left(1 - \frac{k_{\|}^2 c_s^2}{\omega^2} - \frac{\omega_*}{\omega} + 2\frac{\omega_{de}}{\omega}(\cos\theta - \frac{i}{k_\theta}\sin\theta\frac{\partial}{\partial r}) - \rho_s^2(\frac{\partial^2}{\partial r^2} - k_\theta^2)\right)\tilde{\Phi} =$$

$$-\left(1 - \frac{k_{\|}^2 c_s^2}{\omega^2}\right)\delta\tilde{n}_e + \left(i\frac{\beta_n}{\omega} - \frac{i(\gamma_v + \beta_n)k_{\|}^2 c_s^2}{\omega^2(\omega + i\gamma_v + i\beta_n)}\right)\tilde{n}_e + \left(i\frac{\beta_T}{\omega} + \frac{k_{\|}^2 c_s^2}{\omega(\omega + i\gamma_v + i\beta_n)}\right)\tilde{T}. \quad (19)$$

Here we have broken the perturbed electron density into its adiabatic and non-adiabatic parts: $\tilde{n}_e = \tilde{\Phi} + \delta\tilde{n}_e$. The right-hand side of Eq. (19) contains the non-adiabatic electron response and the atomic physics effects. Because the electrons are nearly adiabatic and atomic physics effects are small for typical TEXT and TFTR parameters considered here, we treat the right hand side of Eq. (19) perturbatively.

We use the usual (r, θ, ξ) coordinates, corresponding to the minor radial, poloidal, and toroidal directions. In a large aspect-ratio axisymmetric torus, the perturbed potential can be expressed as:

$$\tilde{\Phi}(r, \theta, \xi) = \sum_j \hat{\Phi}_j(s) \exp[i(m_0\theta + j\theta - n\xi - \omega t)], \tag{20}$$

where $|j| \ll m_0$, $s = \frac{(r-r_0)}{\Delta r_s}$, r_0 is the reference rational surface $m_0 = nq(r_0)$, $\Delta r_s = \frac{1}{k_\theta \hat{s}}$, $k_\theta = \frac{m_0}{r_0}$, and $\hat{s} = \frac{rq'}{q}$ at $r = r_0$. Ignoring for the moment the right-hand side, Eq. (19) is:

$$\left[1 - \frac{1}{\Omega} - \frac{(s-j)^2}{\eta_s^2\Omega^2} - b_\theta(\hat{s}^2\frac{\partial^2}{\partial s^2} - 1)\right]\hat{\Phi}_j + \frac{\epsilon_n}{\Omega}\left[\hat{\Phi}_{j-1} + \hat{\Phi}_{j+1} - \hat{s}\frac{\partial}{\partial s}(\hat{\Phi}_{j-1} - \hat{\Phi}_{j+1})\right] = 0 \tag{21}$$

where we have used $k_\| = \frac{(s-j)}{qR}$, $b_\theta = k_\theta^2\rho_s^2$, $\Omega = \frac{\omega}{\omega_*}$, $\eta_s = \frac{qb_\theta^{\frac{1}{2}}}{\epsilon_n}$, $\epsilon_n = \frac{L_n}{R}$. Using the ballooning mode formalism, for $|m_0| \sim |n| \gg 1$, $\hat{\Phi}_j(s) = \Phi(z)$, and $\hat{\Phi}_{j\pm1}(s) = \Phi(z \mp 1)$, with $z = s - j$. In this approximation, the eigenmodes are composed of identical structures centered at each rational surface. The eigenmode equation is:

$$\left[1 - \frac{1}{\Omega} - \frac{z^2}{\eta_s^2\Omega^2} - b_\theta(\hat{s}^2\frac{d^2}{dz^2} - 1)\right]\Phi(z) + \frac{\epsilon_n}{\Omega}\left[\Phi(z+1) + \Phi(z-1) - \hat{s}\frac{d}{dz}[\Phi(z+1) - \Phi(z-1)]\right] = 0 \tag{22}$$

We now Fourier transform this equation:

$$\Phi(\eta) = \int_{-\infty}^{\infty} dz\, e^{i\eta z}\, \Phi(z). \tag{23}$$

The eigenmode equation is now a one-dimensional differential equation in the ballooning coordinate, η:[14]

$$\left[\frac{d^2}{d\eta^2} + Q(\eta, \Omega)\right]\Phi(\eta) = 0, \tag{24a}$$

where

$$Q(\eta, \Omega) = \eta_s^2\Omega^2\left[1 - \frac{1}{\Omega} + b_\theta(1 + \hat{s}^2\eta^2) + \frac{2\epsilon_n}{\Omega}(\cos\eta + \hat{s}\eta\sin\eta)\right]. \tag{24b}$$

The $\frac{d^2}{d\eta^2}$ term is the ion sound wave contibution. In the expression for Q, 1 is the Boltzmann electron response, $-\frac{1}{\Omega}$ is the $\mathbf{E} \times \mathbf{B}$ convection of the ion density, $\hat{s}^2\eta^2$ is the ion polarization drift, and $\frac{2\epsilon_n}{\Omega}(\cos\eta + \hat{s}\eta \sin\eta)$ is the toroidal coupling term. We repeat this procedure including the right-hand side of Eq. (19), and obtain:

$$\left[\frac{d^2}{d\eta^2} + Q(\eta,\Omega) + \delta Q(\eta,\Omega)\right]\Phi(\eta) = 0, \tag{25a}$$

$$\begin{aligned}\delta Q(\eta,\Omega) = \frac{\eta_s^2\Omega^2}{\Phi(\eta)}\int_{-\infty}^{\infty} dz\, e^{i\eta z}\,\Phi(z)&\left[\left(1 - \frac{z^2}{\eta_s^2\Omega^2}\right)\delta\tilde{n}_e\right.\\ -i\left(\frac{\frac{\beta_n}{\omega_*}}{\Omega} - \frac{\frac{\gamma_v}{\omega_*} + \frac{\beta_n}{\omega_*}}{\Omega + i\frac{\gamma_v}{\omega_*} + i\frac{\beta_n}{\omega_*}}\frac{z^2}{\eta_s^2\Omega^2}\right)\tilde{n}_e &\left. - \left(\frac{i\frac{\beta_T}{\omega_*}}{\Omega} + \frac{\Omega}{\Omega + i\frac{\gamma_v}{\omega_*} + i\frac{\beta_n}{\omega_*}}\frac{z^2}{\eta_s^2\Omega^2}\right)\tilde{T}\right],\end{aligned} \tag{25b}$$

where $\Phi(z) = \frac{1}{2\pi}\int_{-\infty}^{\infty} dz\, e^{-i\eta z}\,\Phi(\eta)$.

We solve this equation as follows. First, we find the lowest order eigenfunction using adiabatic electrons ($\delta Q = 0$). Then using this lowest order eigenfunction, we evaluate $\delta Q(\eta)$ in Eq. (25b). We find that $\delta Q(\eta)$ is constant over the eigenmode $\Phi(\eta)$ to a very good approximation. For small and constant δQ, the effect on stability is simply $\text{Im}(\omega/\omega_*) \simeq -\text{Im}(\delta Q)/\eta_s^2\Omega^2$. As far as linear anaylsis is concerned, TFTR and TEXT parameters justify the perturbative treatment, since $\gamma \ll \omega_r$, as will be shown. Equation (24) is the eigenmode equation of Ref. 14, and is obtained from our equations neglecting the non-adiabatic electron response and atomic physics. We solve Eq. (24) numerically using an interactive WKB shooting code.[20] We are interested in the most unstable modes for this system, which are the neutrally stable toroidicity induced eigenmodes. Figures 1 and 2 show numerical solutions to this equation for typical tokamak parameters, for an extremely long wavelength eigenmode, $k_\theta\rho_s = 0.02$ (Fig. 1), and for a shorter wavelength eigenmode, $k_\theta\rho_s = 0.1$ (Fig. 2). The effective potential, $-Q(\eta)$, is shown in (a). The toroidal coupling terms create the local potential well which makes the magnetic shear induced damping ineffective, thus making these modes neutrally stable. The eigenmode structure in the ballooning coordinate, $\Phi(\eta)$, is shown in (b). The eigenmode structure in the radial coordinate, $\Phi(z)$, obtained by Fourier tranforming $\Phi(\eta)$, is shown in (c). The eigenfrequencies for these two cases are $\Omega = 0.82$ for $k_\theta \rho_s = 0.02$ and $\Omega = 0.48$ for $k_\theta \rho_s = 0.1$.

To proceed, we solve Eqs. (9)-(11) and (13) for $\tilde{n}_e$, $\delta\tilde{n}_e$, and $\tilde{T}$ in terms of $\tilde{\Phi}$, and obtain:

$$\tilde{n}_e = \frac{ae + bf}{ad - cf}\tilde{\Phi} \qquad \tilde{T} = \frac{bd + ce}{ad - cf}\tilde{\Phi} \tag{26}$$

$$\delta\tilde{n}_e = \frac{a(e-d) + (b+c)f}{ad - cf}\tilde{\Phi}$$

where:

$$\begin{aligned}
a &= i\frac{2}{3}(3.16 + \frac{(1.71)^2}{0.51})\frac{x^2}{\overline{\nu}\Omega} - \frac{2}{3}\frac{x^2}{\Omega(\Omega + i\frac{\gamma_v}{\omega_*} + i\frac{\beta_n}{\omega_*})} + 1 + i(\frac{\gamma_T}{\omega} + \frac{2}{3}\frac{\beta_n}{\omega} + \frac{2}{3}\frac{\beta_T}{\omega}) \qquad (27)\\
b &= i\frac{2}{3}\frac{1.71}{0.51}\frac{x^2}{\overline{\nu}\Omega} + \frac{\eta_e}{\Omega}\\
c &= -i\frac{2}{3}\frac{1.71}{0.51}\frac{x^2}{\overline{\nu}\Omega} + \frac{2}{3}\frac{x^2}{\Omega(\Omega + i\frac{\gamma_v}{\omega_*} + i\frac{\beta_n}{\omega_*})} - i(\frac{\gamma_n}{\omega} + \frac{2}{3}\frac{\beta_n}{\omega})\\
d &= i\frac{x^2}{0.51\,\overline{\nu}\Omega} - \frac{x^2}{\Omega(\Omega + i\frac{\gamma_v}{\omega_*} + i\frac{\beta_n}{\omega_*})} + 1 - i\frac{\beta_n}{\omega}\\
e &= i\frac{x^2}{0.51\,\overline{\nu}\Omega} + \frac{1}{\Omega}\\
f &= -i\frac{1.71}{0.51}\frac{x^2}{\overline{\nu}\Omega} + \frac{x^2}{\Omega(\Omega + i\frac{\gamma_v}{\omega_*} + i\frac{\beta_n}{\omega_*})} + i\frac{\beta_T}{\omega}.
\end{aligned}$$

We have normalized $z = x\eta_s$, and $\overline{\nu} = \frac{\nu_{ei} m_e}{\omega_* m_i}$. These terms in δQ are ratios of fourth order polynomials in z, and do not Fourier transform nicely into ballooning space as the z^2 and $\frac{d^2}{dz^2}$ terms do in the unperturbed eigenmode equation, so we evaluate them in configuration space, and then transform to ballooning space.

Typical edge parameters for TFTR and TEXT are shown in Table I. γ_n is calculated using experimentally measured P_{rad}. To estimate γ_T, we use coronal equilibrium cooling rates,[21] normalized to match P_{rad}. Since the actual $L_z(T_e)$ will be smoother than the coronal model, this is an upper bound on γ_T. All atomic physics rates are much smaller than ω_* for m values of interest. Using the lowest order eigenfunctions, we can now evaluate $\frac{k_\parallel^2 v_{te}^2}{\omega\nu_{ei}}$ and $\frac{k_\parallel^2 c_s^2}{\omega^2}$, and identify the parameter regime for these fluctuations. For the toroidicity induced modes, $k_\parallel \sim \frac{\Delta x}{L_s} k_\theta$, where $\Delta x \sim \frac{1}{k_\theta \hat{s}}$ and $L_s = \frac{qR}{\hat{s}}$, so

$$\frac{k_\parallel^2 c_s^2}{\omega^2} \sim \left(\frac{L_n}{qR}\right)^2 \left(\frac{\omega_*}{\omega}\right)^2 \frac{1}{(k_\theta \rho_s)^2}. \tag{28}$$

In the TFTR and TEXT edge, this quantity varies from 10^{-3} for short wavelengths ($k_\theta \rho_s = 1$) to 1 for longer wavelengths ($k_\theta \rho_s = 0.05$). Therefore, we have $\frac{k_\parallel^2 c_s^2}{\omega^2} \lesssim 1$ for parameters of interest, and pressure balance is not likely to be achieved, even for rather low $k_\theta \rho_s$ ($m \sim 50$).

More importantly, since

$$\frac{k_\parallel^2 v_{te}^2}{\omega \nu_{ei}} = \frac{1}{\overline{\nu}} \frac{k_\parallel^2 c_s^2}{\omega^2} \frac{\omega}{\omega_*}, \tag{29}$$

and typically $\overline{\nu} \ll 1$, even for rather low $k_\theta \rho_s$, we have $\frac{k_\parallel^2 v_{te}^2}{\omega\nu_{ei}} \gg 1 \gtrsim \frac{k_\parallel^2 c_s^2}{\omega^2}$. In summary, these fluctuations are typically in the adiabatic regime.

Because of the spatial dependence of $k_\parallel$, the electrons are hydrodynamic only within a narrow region near the rational surface, and adiabatic outside this region, as shown in Fig. 3. For illustration, Fig. 4 shows the case $\overline{\nu} \gg 1$, where the electrons are hydrodynamic near the rational surface, and pressure balance is enforced outside this region. The typical parameter regimes for toroidal drift waves in TFTR and TEXT are shown in Fig. 5.

We can now evaluate the integral for δQ using the lowest order eigenfunctions $\Phi(z)$, as shown in Figs. 1(c) and 2(c), for example. Since $\overline{\nu} \ll 1$, the electrons are non-adiabatic only within a narrow region near the rational surface, and the integrand for the perturbed potential δQ looks like a delta function in z. When transformed into ballooning space, $\delta Q(\eta)$ is roughly constant over the width of the eigenmode, as shown for these two cases in Figs. 6 and 7.

If the atomic physics rates are η-dependent due to specific experimental situations such as the limiter configuration and gas puff location, the imaginary (dissipative) part of δQ would be η-dependent and could induce toroidal coupling.[22] For the parameters considered in this paper, the toroidal coupling in the real (reactive) part of Q caused by ion drifts is a larger effect since $\omega_{de} \gg \gamma$.

In the limit $\overline{\nu} \ll 1$, we can evaluate δQ analytically without knowing the detailed eigenmode structure, keeping terms up to $O(\overline{\nu}^{\frac{1}{2}})$. The lowest order piece of the $\delta\tilde{n}_e$ term in Eq. (25b) contributes

$$\begin{aligned}\delta Q \;=\;& \eta_s^3\overline{\nu}^{\frac{1}{2}}\Omega^{\frac{3}{2}}\frac{\sqrt{\pi}}{2}(1-i)\;\; [2.51(1-\Omega) - 1.06\,\eta_e] \\ &+\eta_s^3\overline{\nu}^{\frac{1}{2}}\Omega^{\frac{1}{2}}\frac{\sqrt{\pi}}{2}(1+i)[\;\; \frac{\gamma_T}{\omega_*}(0.24\,\Omega + 0.33(1-\Omega) + 0.19\,\eta_e) \\ &+ \frac{\gamma_n}{\omega_*}(1.13\,\Omega + 0.49(1-\Omega) - 0.16\,\eta_e) \\ &+ \frac{\beta_T}{\omega_*}(0.35\,\Omega + 0.02(1-\Omega) + 0.87\,\eta_e)\,]\,.\end{aligned} \tag{30}$$

For the second term in Eq. (25b), $\tilde{n}_e = \tilde{\Phi}$ to lowest order. The β_n term is trivial to evaluate, but for the γ_v term we approximate $\int_{-\infty}^{\infty} z^2\,\Phi(z)\,dz \simeq \frac{2}{\pi^2}$. The dominant contribution is:

$$\delta Q = -i\eta_s^2\Omega^2\frac{\beta_n}{\omega} + i\frac{2}{\pi^2}(\frac{\gamma_v}{\omega} + \frac{\beta_n}{\omega}). \tag{31}$$

The lowest order contribution from the $\tilde{T}$ term is proportional to $\frac{\beta_T}{\omega_*}$:

$$\delta Q = \eta_s^3\overline{\nu}^{\frac{1}{2}}\Omega^{\frac{1}{2}}\frac{\sqrt{\pi}}{2}(1+i)\frac{\beta_T}{\omega_*}(0.35\,\Omega + 0.16(1-\Omega) - 0.14\,\eta_e). \tag{32}$$

Combining these terms, the growth rate is:

$$\begin{aligned}\frac{\gamma}{\omega_*} \;=\;& \frac{\beta_n}{\omega} - \frac{2}{\pi^2\eta_s^2\Omega^2}(\frac{\gamma_v}{\omega} + \frac{\beta_n}{\omega}) + \frac{\sqrt{\pi}}{2}\eta_s(\frac{\overline{\nu}}{\Omega})^{\frac{1}{2}}\,[2.51\,(1-\Omega) - 1.06\,\eta_e] \\ &-\frac{\sqrt{\pi}}{2}\eta_s(\frac{\overline{\nu}}{\Omega})^{\frac{1}{2}}\,[\;\frac{\gamma_T}{\omega}(0.24\,\Omega + 0.33(1-\Omega) + 0.19\,\eta_e)\end{aligned} \tag{33}$$

$$+\frac{\gamma_n}{\omega}(1.13\,\Omega + 0.49(1-\Omega) - 0.16\,\eta_e)$$
$$+\frac{\beta_T}{\omega}(0.69\,\Omega + 0.17(1-\Omega) + 0.74\,\eta_e)\,].$$

The basic trends of the local analysis remain, with some important modifications. The destabilization from the ionization term in the ion continuity equation is reduced by charge-exchange and ionization drag on the ion velocity, but the stabilizing term is smaller by a factor of $\frac{2}{\pi^2\eta_s^2\Omega^2}$, which depends on the wavelength ($\eta_s \sim k_\theta\rho_s$). As $k_\theta\rho_s$ gets smaller, the stabilizing term becomes competitive. In the third term, the collisional effects scale like $\overline{\nu}^{\frac{1}{2}}$ instead of $\overline{\nu}$ predicted from local theory. Therefore, this term is not negligible compared to $\overline{\nu}$-independent terms. The radiation effects are very weak, since $\overline{\nu}$, γ_n, and γ_T are all small.

Figures 8(a)-(g) compare the numerical and analytical growth rates as $\overline{\nu}$, η_e, β_n, β_T, γ_v, γ_n, and γ_T are varied, using the parameters in Fig. 1.

Typically, the growth rate is determined by the competition between ionization and collisions, the latter is stabilizing for large η_e, and overall stability is achieved when:

$$\eta_e > \eta_{crit} = 2.37(1-\Omega) + \frac{2}{\sqrt{\pi}}\frac{\beta_n}{\omega_*}\frac{1}{(\overline{\nu}\Omega)^{\frac{1}{2}}}\frac{1}{\eta_s}. \tag{34}$$

For the cases considered in Table I, collisional stabilization is stronger than the destabilization from ionization, rendering these modes stable. However, at the extreme edge of tokamaks, steeper density gradients and higher ionization rates may make these modes unstable.

IV Conclusions and Discussion

This paper has focused on the effects of various atomic physics processes on dissipative drift wave stability in toroidal geometry. The principal conclusions of this paper are as follows.

i). For typical parameters of the TFTR and TEXT edge, the electron dynamics are nearly adiabatic.

ii). The deviation from the adiabatic response which is required for instability comes from ionization, collisions, charge exchange, and radiation, roughly in order of importance.

iii). For an instability, the inverse dissipation from ionization or from the downshift of the real frequency below ω_{*e} should overcome the stabilizing effects due to the electron temperature gradient, quantified by η_e. Therefore, for long wavelength modes, an instability is likely to occur at the extreme edge in minor radius with significant ionization source and rather steep electron density gradient (low η_e).

iv). Ionization acts as an inverse dissipation in the density continuity equation, but also appears as an effective drag in the ion *velocity* equation. This effect, although ignored in previous studies,[13] can quantitatively affect stability if $\frac{k_\parallel^2 c_s^2}{\omega^2} \gtrsim 1$.

v). The magnitudes of two dimensionless parameters, $\frac{k_\parallel^2 v_{te}^2}{\omega \nu_{ei}}$ and $\frac{k_\parallel^2 c_s^2}{\omega^2}$ determine the asymptotic regimes in parameter space and the characteristics of the fluctuations. Relevances of the previous studies[11,12,16] on radiation-driven edge turbulence models are discussed for certain regimes.

The detailed linear analyses and results presented in this paper indicate that the edge drift instability has a growth rate which is smaller than the real frequency for $m > 10$. However, we would like to point our that this does not necessarily imply small fluctuation levels at saturation. Since the longer wavelength fluctuations (with $k_\perp \rho_s \ll 1$) are more likely to be destabilized by the ionization, the weak turbulence analysis based upon nonlinear wave-particle interactions (including ion Compton scattering) is not likely to be justified. In the strong turbulence regime, the Hasegawa-Mima nonlinearity[23] is also negligible because it relies on the nonlinear polarization drift. Therefore, the nonlinear saturation could occur through a nonlinear process which is insensitive to the strength of finite Larmor radius effects. One possibility would be the dissipative correction to $\mathbf{E} \times \mathbf{B}$ convection.[24] Since this nonlinearity is also weak, it is possible to have a large fluctuation level at saturation.[13]

Acknowledgments

We would like to thank G. W. Hammett for pointing out important modifications to the Braginskii equations, and R. Budny and W. L. Rowan for providing the experimental data. We also thank P. H. Diamond for useful sugges 'ons.

This work was supported by a National Science Foundation Fellowship and by the United States Department of Energy contract No. DE-AC02-76-CHO-3703.

References

[1] S. J. Zweben and R. W. Gould, Nucl. Fusion **23**, 1625 (1983).

[2] Ch. P. Ritz, R. D. Bengston, S. J. Levinson, and E. J. Powers, Phys. Fluids **27**, 2956 (1984).

[3] A. J. Wootton, B. A. Carreras, H. Matsumoto, K. McGuire, W. A. Peebles, Ch. P. Ritz, P. W. Terry, and S. J. Zweben, Phys. Fluids B **2**, 2879 (1990).

[4] P. W. Terry and P. H. Diamond, Phys. Fluids **28**, 1419 (1985).

[5] L. Garcia, P. H. Diamond, B. A. Carreras, and J. D. Callen, Phys. Fluids **28**, 2147 (1985).

[6] H. P. Furth, J. Killeen, and M. N. Rosenbluth, Phys. Fluids **6**, (1963).

[7] K. W. Gentle, R. D. Bengston, R. Bravenec, D. L. Brower, W. L. Hodge, T. P. Kochanski, N. C. Luhmann, D. Patterson, W. S. Peebles, and P. E. Phillips, Plasma Phys. **26**, 1407 (1984).

[8] M. C. Zarnstorff, R. J. Goldston, E. Fredrickson, C. Bush, B. Grek, T. S. Hahm, D. Johnson, D. Mansfield, D. McCune, H. Park, A. Ramsey, J. Schivell, and G. Taylor, in Proceedings of Annual Controlled Fusion Theory Conference (San Antonio, Texas, 1989).

[9] P. H. Rutherford, in *Physics of Plasma Close to Thermonuclear Conditions*, edited by B. Coppi, et. al. (Pergamon, New York, 1981), Vol. I, p. 143.

[10] T. S. Hahm, P. H. Diamond, P. W. Terry, L. Garcia, and B. A. Carreras, Phys. Fluids **30**, 1452 (1987).

[11] D. R. Thayer and P. H. Diamond, Phys. Fluids **30**, 3724 (1987).

[12] A. S. Ware, P. H. Diamond, B. A. Carreras, J. N. Leboeuf, and D. K. Lee, Phys. Fluids B **4**, 102 (1992).

[13] A. S. Ware, P. H. Diamond, H. Biglari, B. A. Carreras, L. A. Charlton, J.-N. Leboeuf, A. J. Wootton, (submitted to Phys. Fluids B).

[14] L. Chen and C. Z. Cheng, Phys. Fluids **23**, 2242 (1980).

[15] S. I. Braginskii, in Reviews of Plasma Physics, edited by M. A. Leontovich (Consultants Bureau, New York, 1965), Vol. I, p. 205.

[16] J. F. Drake, L. Sparks, and G. Van Hoven, Phys. Fluids **31**, 813 (1988).

[17] J. W. Connor, R. J. Hastie, and J. B. Taylor, Proc. R. Soc. **365**, 1 (1979).

[18] A. H. Glasser, in *Proceedings of the Finite Beta Theory Workshop*, Varenna, 1977, edited by B. Coppi and W. Sadowski (U. S. Department of Energy, CONF-7709167, 1977), p. 55.

[19] Y. C. Lee and J. W. Van Dam, in *Proceedings of the Finite Beta Theory Workshop*, Varenna, 1977, edited by B. Coppi and W. Sadowski (U. S. Department of Energy, CONF-7709167, 1977), p. 93.

[20] R. B. White, J. Comput. Phys. **31**, 409 (1979).

[21] D. E. Post, R. V. Jensen, C. B. Tarter, W. H. Grasberger, and W. A. Lokke, At. Data Nucl. Data Tables **20**, 397 (1977).

[22] A. S. Ware and P. H. Diamond, private communication, 1991.

[23] A. Hasegawa and K. Mima, Phys. Rev. Lett. **39**, 205 (1977).

[24] B. B. Kadomtsev and O. P. Pogutse, Sov. Phys. JETP **24**, 1172 (1967).

Table I. Typical Edge Parameters

r=0.95 a

	TFTR	TEXT
n_e (cm^{-3})	8×10^{12}	8×10^{12}
T_e (eV)	150	40
n_N (cm^{-3})	3×10^{9}	3×10^{10}
P_{rad} ($\mathrm{W/cm}^3$)	0.03	0.1
L_n (cm)	10	4
L_T (cm)	5	2
η_e	2	2
a (cm)	80	27
R_0 (cm)	245	100
B_0 (T)	4.5	2
q	4	4
$\hat{s}$	2	2
ϵ_n	.04	.15
c_s (cm/s)	8.5×10^{6}	4.4×10^{6}
ν_{ei} (s^{-1})	1.9×10^{5}	1.4×10^{6}
ρ_s (cm)	3.9×10^{-2}	4.6×10^{-2}
ω_{*e} (s^{-1}) for $k_\theta \rho_s = 0.1$	8.5×10^{4} ($m = 195$)	1.1×10^{5} ($m = 56$)
ω_{*e} (s^{-1}) for $k_\theta \rho_s = 0.02$	1.7×10^{4} ($m = 39$)	2.2×10^{4} ($m = 11$)
β_n (s^{-1})	100	800
β_T (s^{-1})	-10	300
γ_v (s^{-1})	200	1000
γ_n (s^{-1})	100	1300
γ_T (s^{-1})	-200	1400

Figure Captions

Fig. 1. Numerical solution of Eq. (24a) for extremely long wavelength ($k_\theta \rho_s = 0.02$), with $q = 4$, $\epsilon_n = 0.1$, and $\hat{s} = 2$. (a) Effective potential $-Q(\eta)$ in ballooning coordinate. (b) Lowest order eigenmode in ballooning coordinate, $\Phi(\eta)$. (c) Lowest order eigenmode in radial coordinate, $\Phi(z)$.

Fig. 2. Numerical solution of Eq. (24a) for $k_\theta \rho_s = 0.1$, with $q = 4$, $\epsilon_n = 0.1$, and $\hat{s} = 2$. (a) Effective potential $-Q(\eta)$ in ballooning coordinate. (b) Lowest order eigenmode in ballooning coordinate, $\Phi(\eta)$. (c) Lowest order eigenmode in radial coordinate, $\Phi(z)$.

Fig. 3. Spatial dependence of $\tilde{n}$ (solid) and $\tilde{T}$ (dashed) for $\overline{\nu} \ll 1$.

Fig. 4. Spatial dependence of $\tilde{n}$ (solid) and $\tilde{T}$ (dashed) for $\overline{\nu} \gg 1$.

Fig. 5. Typical parameter regimes for toroidal drift waves in TFTR and TEXT (electron response).

Fig. 6. Perturbed potential for eigenmode in Fig. 1.

Fig. 7. Perturbed potential for eigenmode in Fig. 2.

Fig. 8. Comparison of analytically (dashed) and numerically (solid) computed growth rates as (a) $\overline{\nu}$, (b) η_e, (c) β_n, (d) β_T, (e) γ_v, (f) γ_n, and (g) γ_T are varied, using the parameters in Fig. 1.

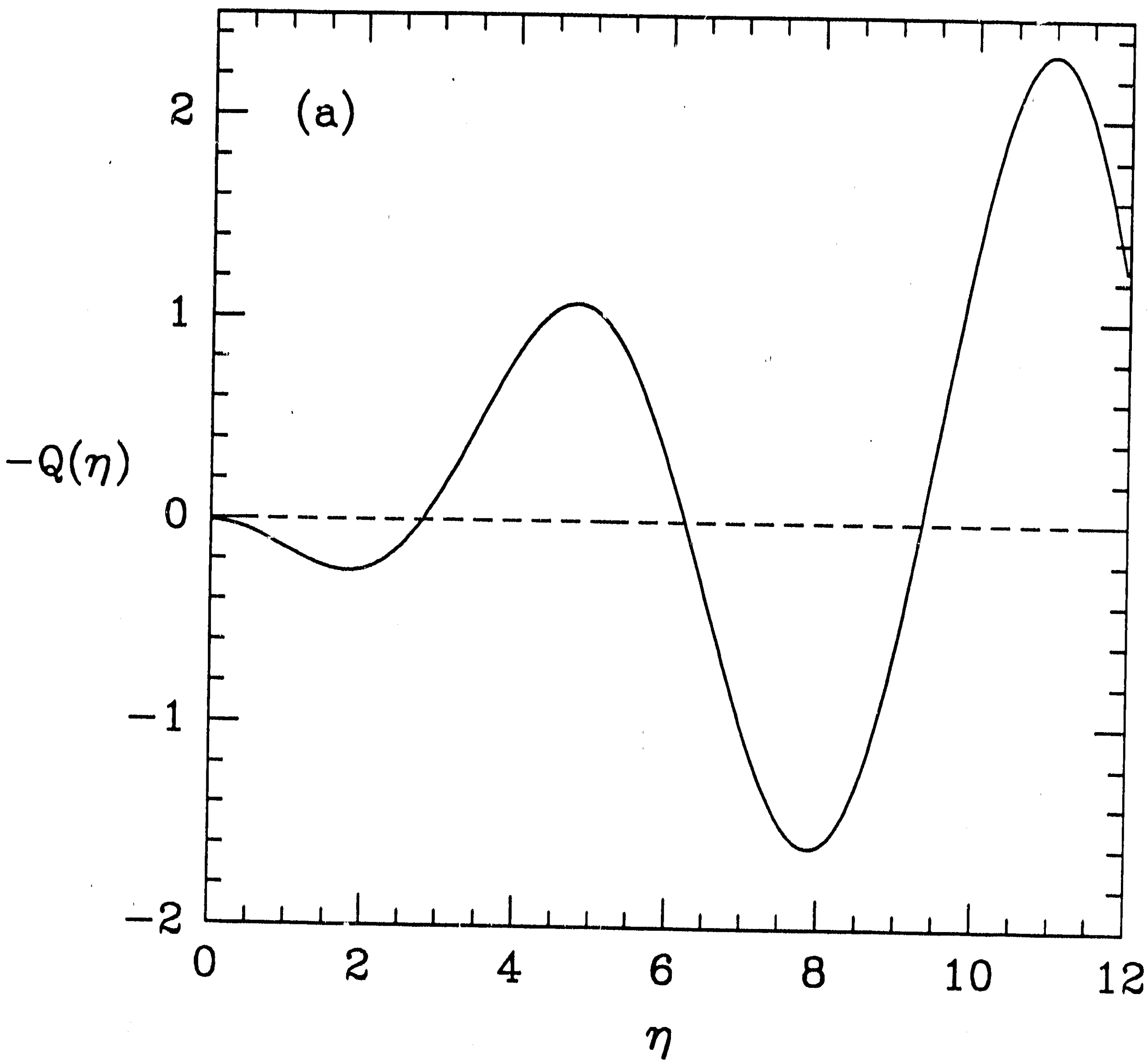

Fig. 1(a).

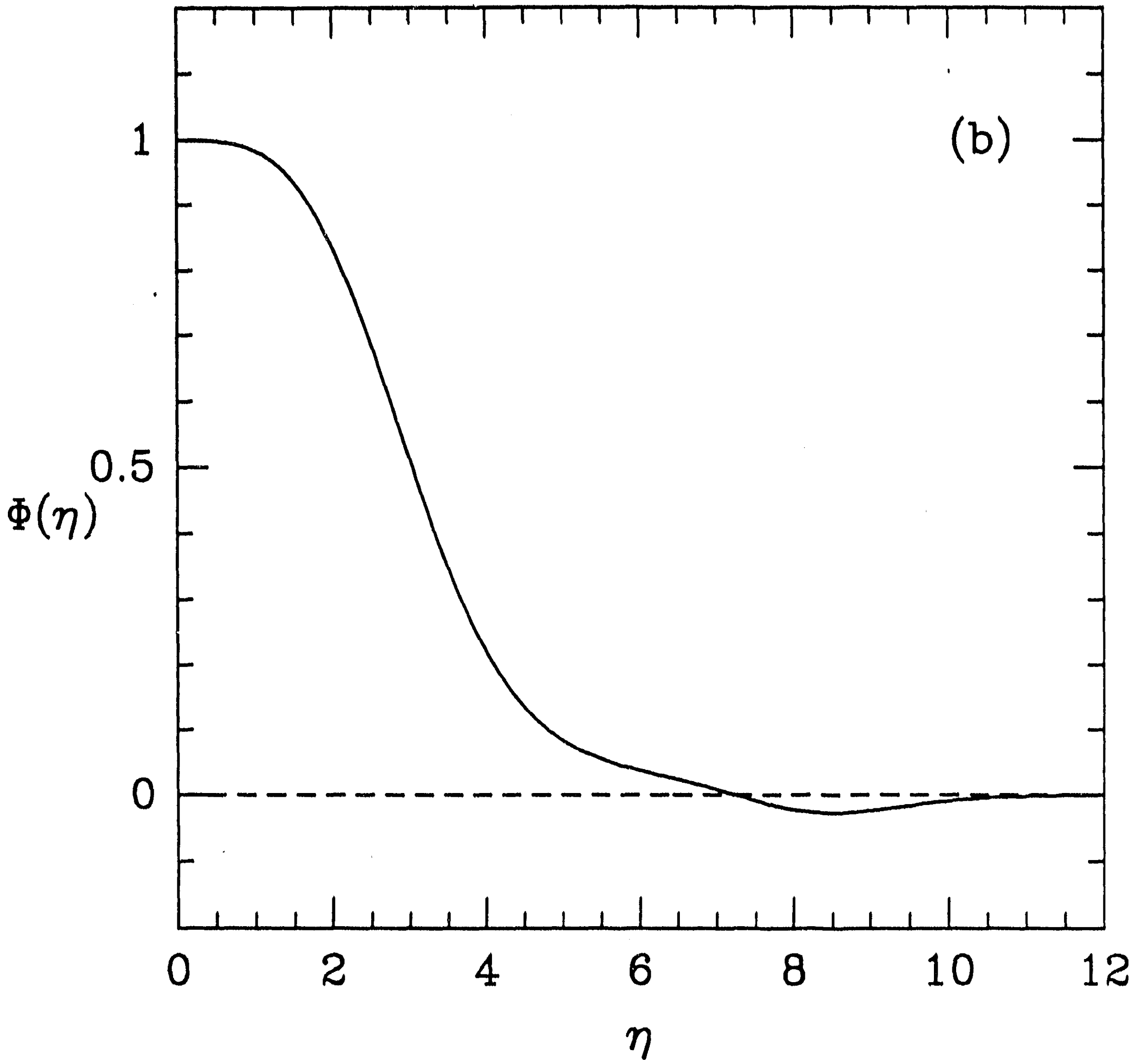

Fig. 1(b).

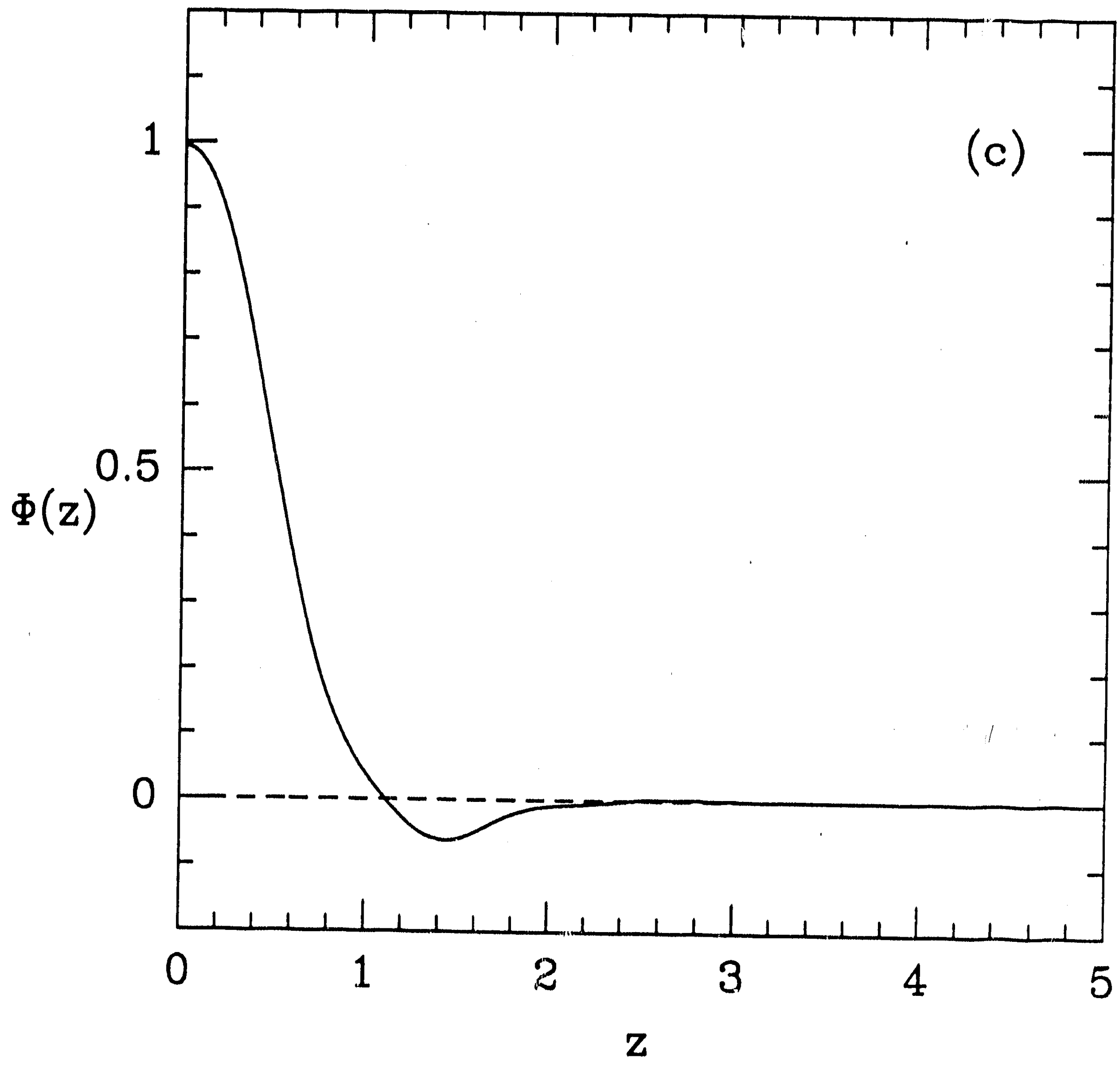

Fig. 1(c).

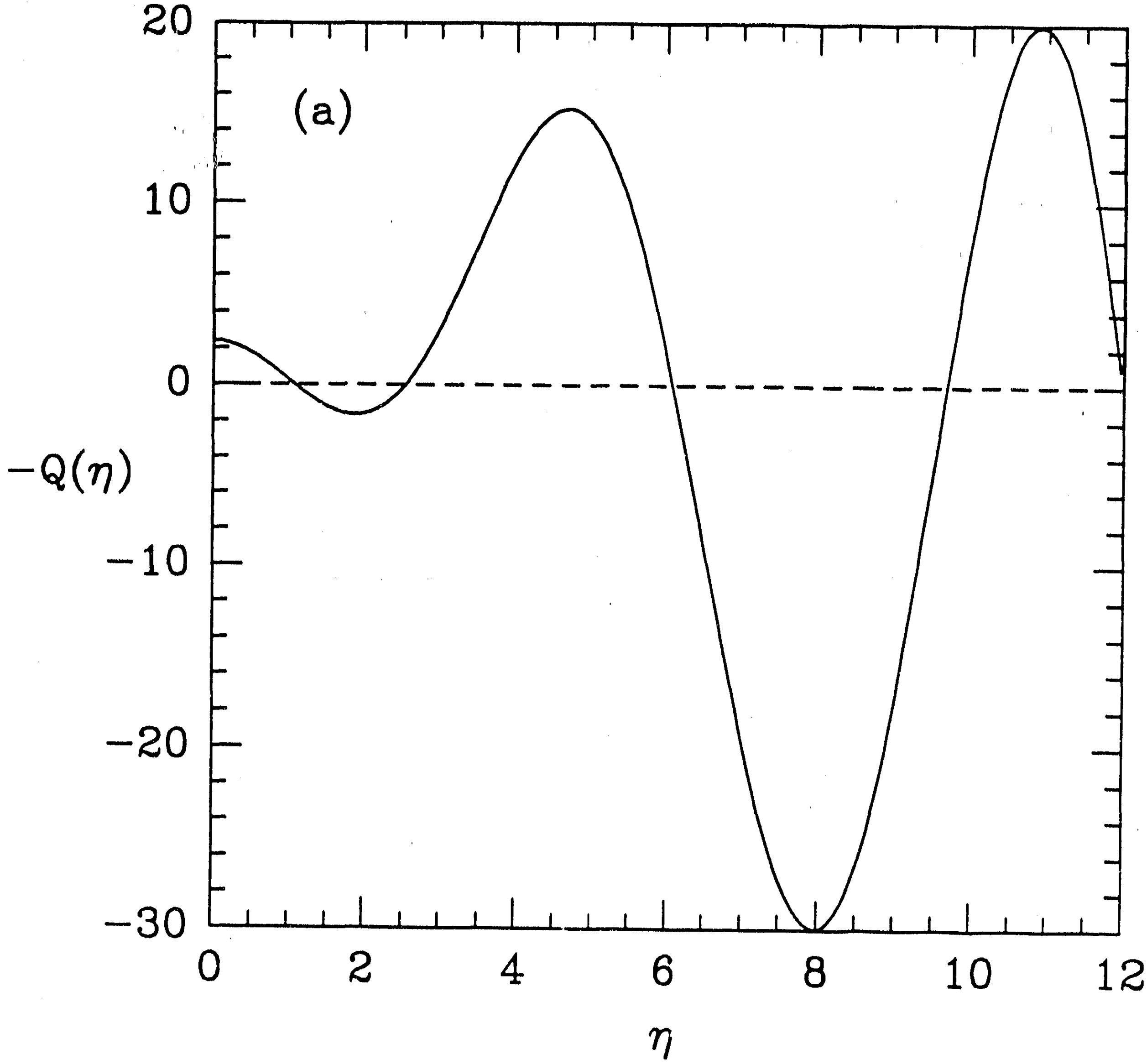

Fig. 2(a).

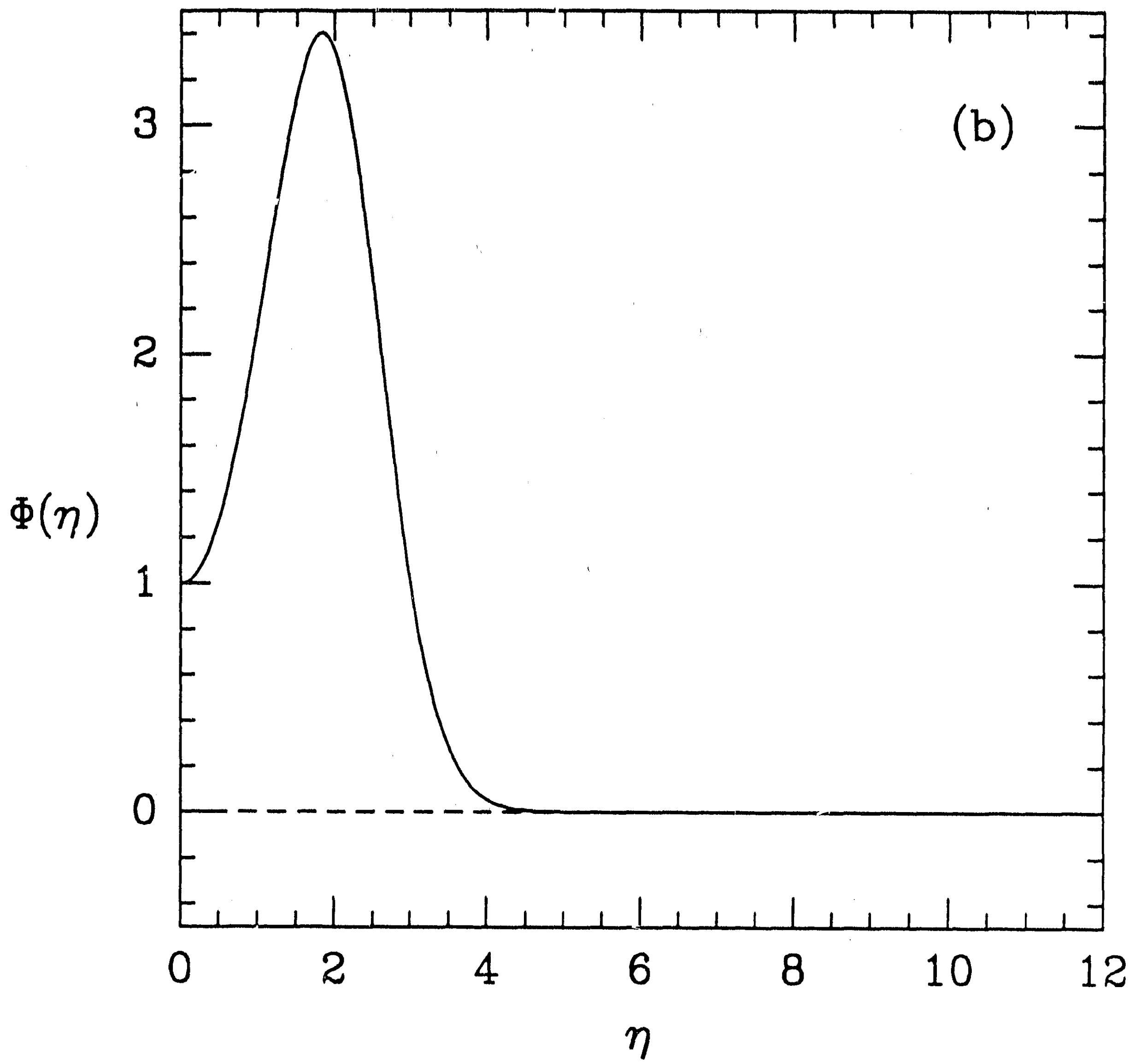

Fig. 2(b).

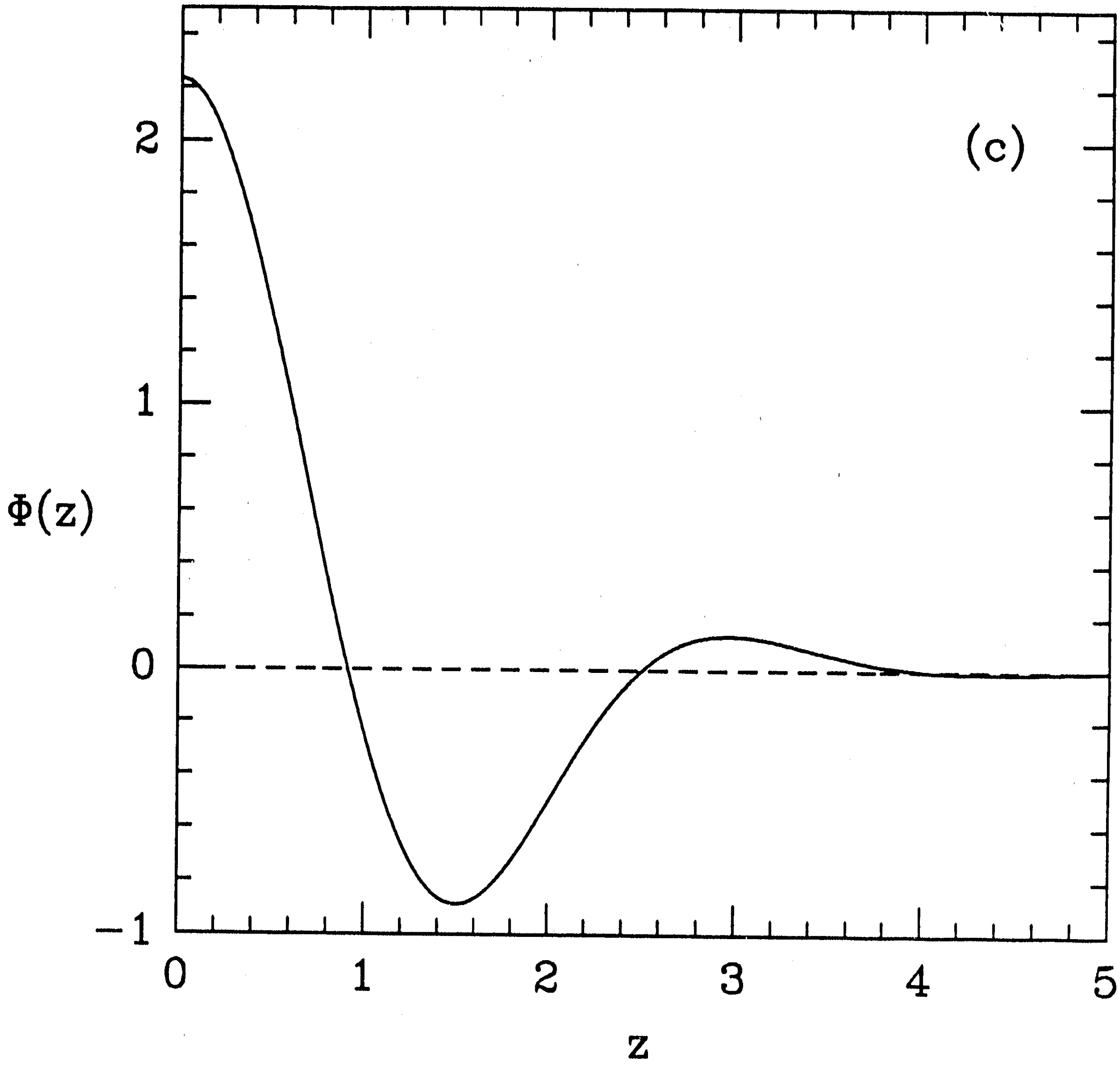

Fig. 2(c).

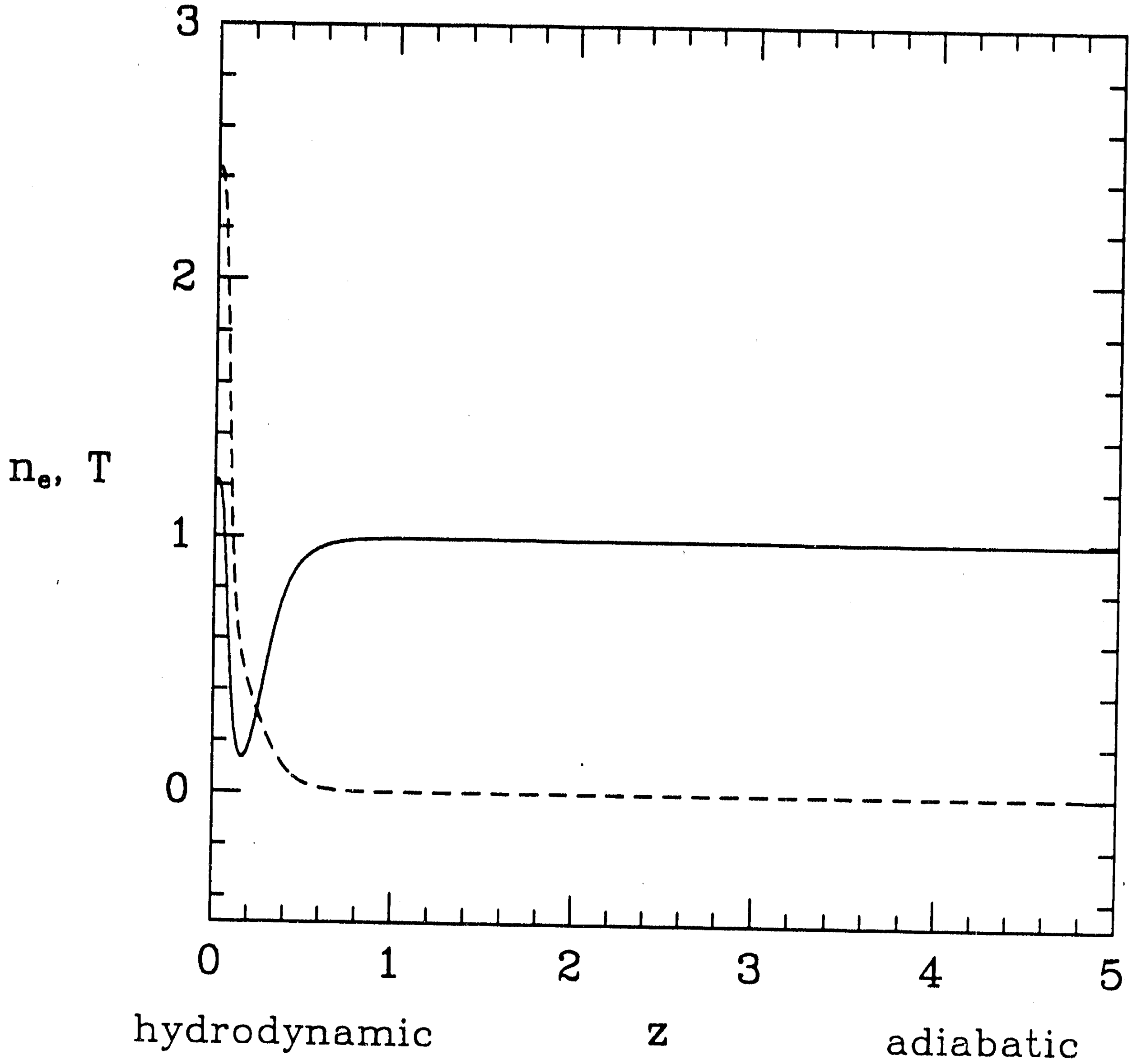

Fig. 3.

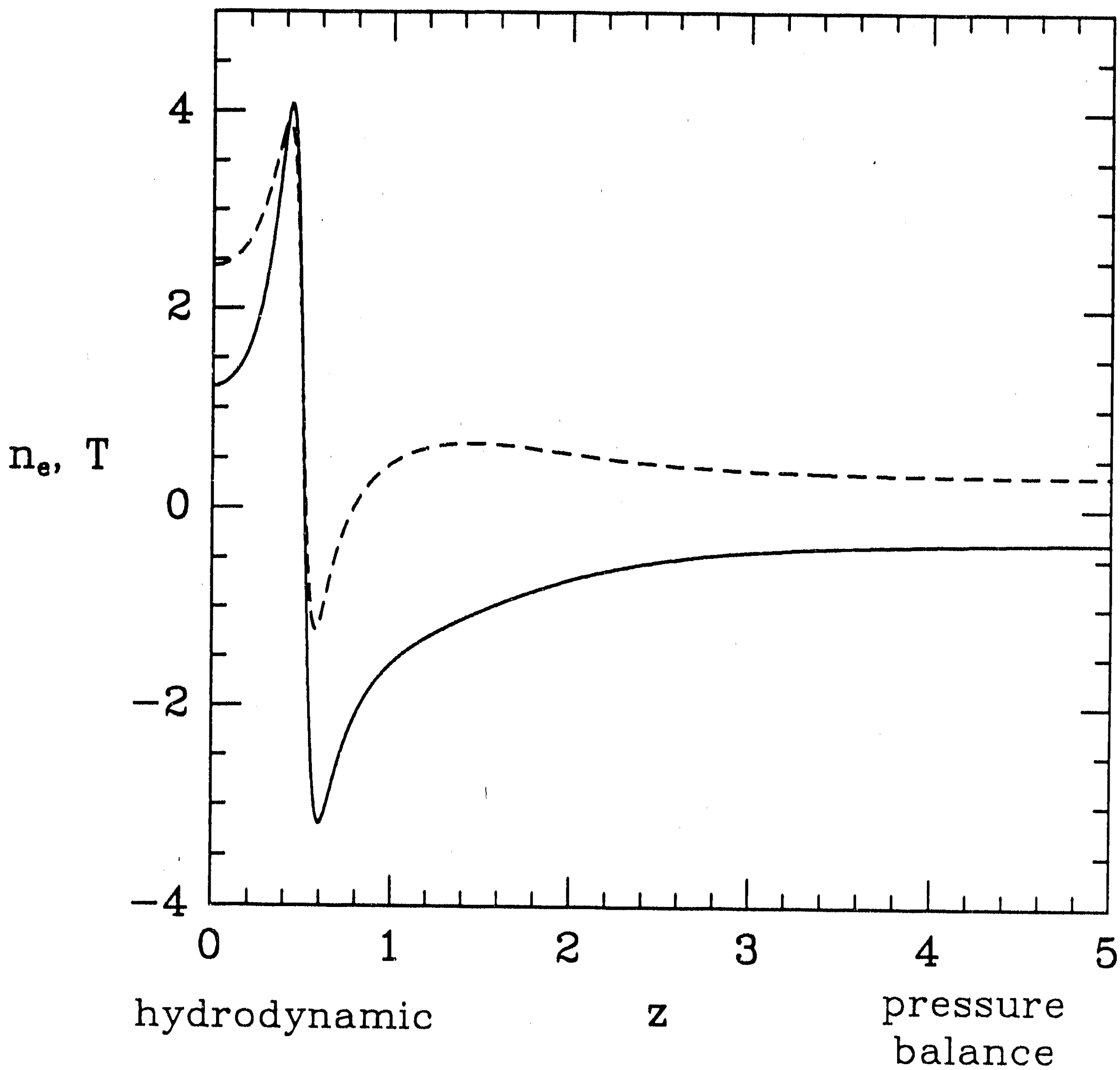

Fig. 4.

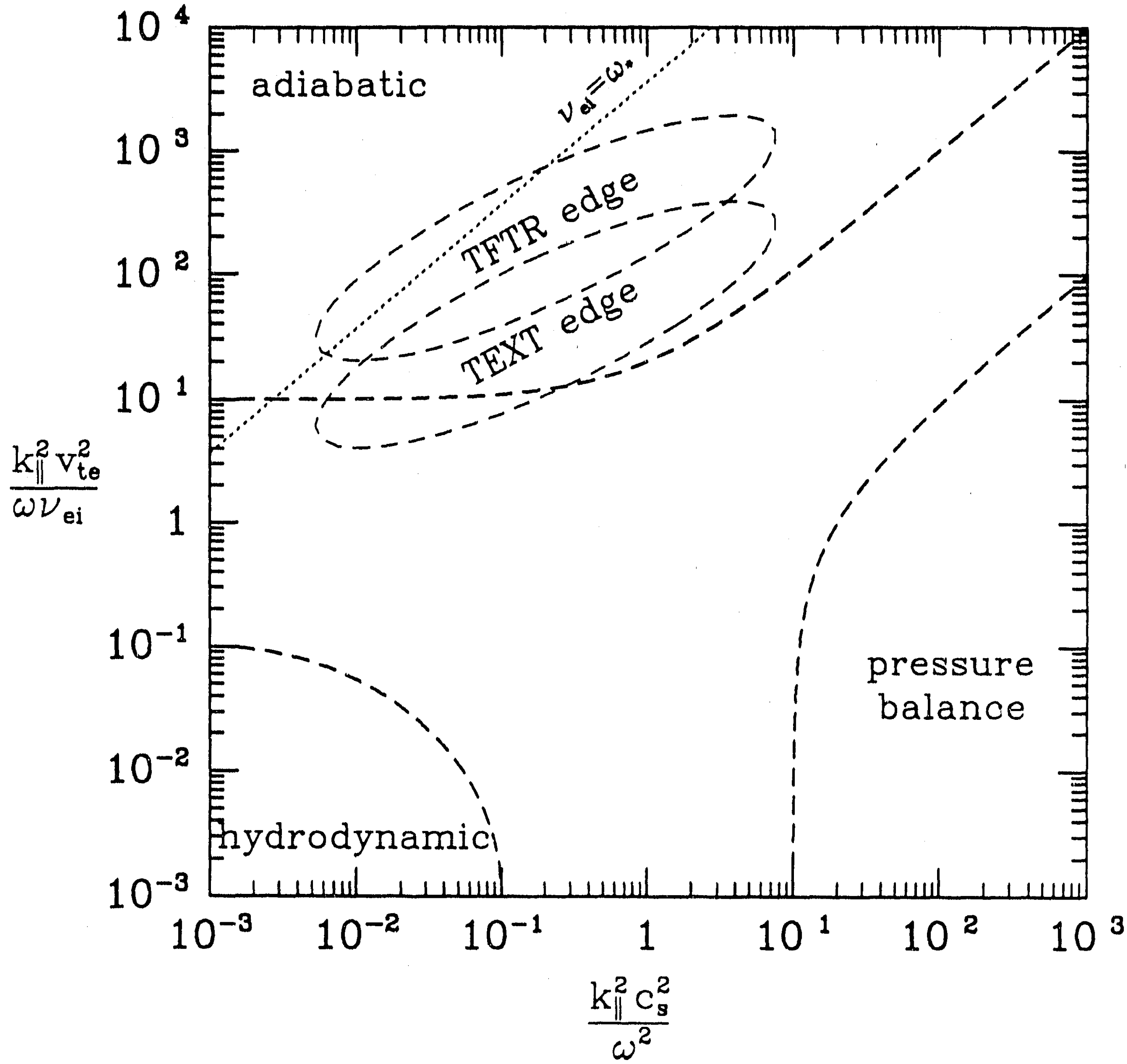

10^4
10^3
10^2
10^1
1
10^{-1}
10^{-2}
10^{-3}
$\frac{k_\parallel^2 v_{te}^2}{\omega \nu_{ei}}$
adiabatic
$\nu_{ei}=\omega_*$
TFTR edge
TEXT edge
pressure balance
hydrodynamic
10^{-3}
10^{-2}
10^{-1}
1
10^1
10^2
10^3
$\frac{k_\parallel^2 c_s^2}{\omega^2}$

Fig. 5.

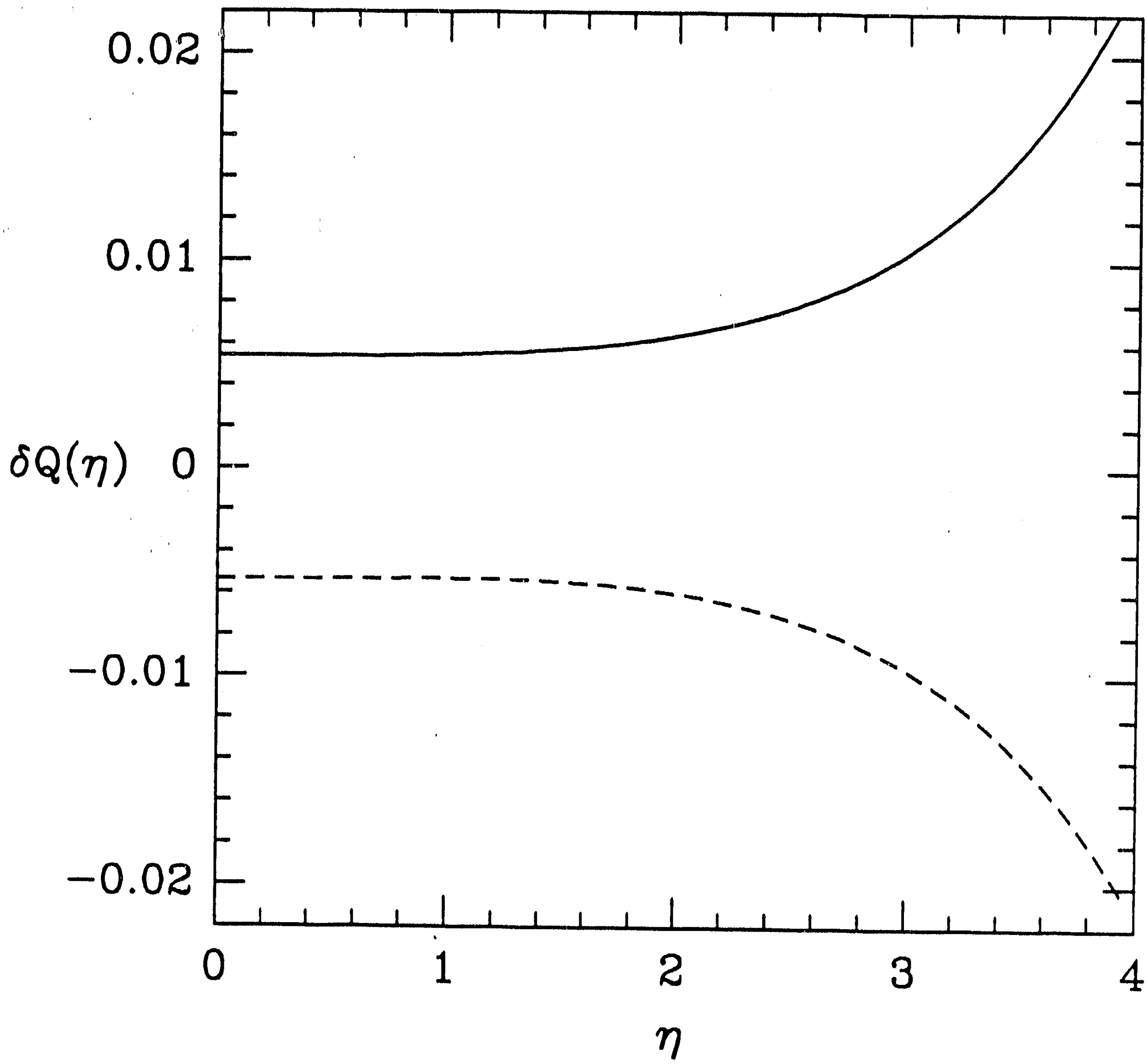

Fig. 6.

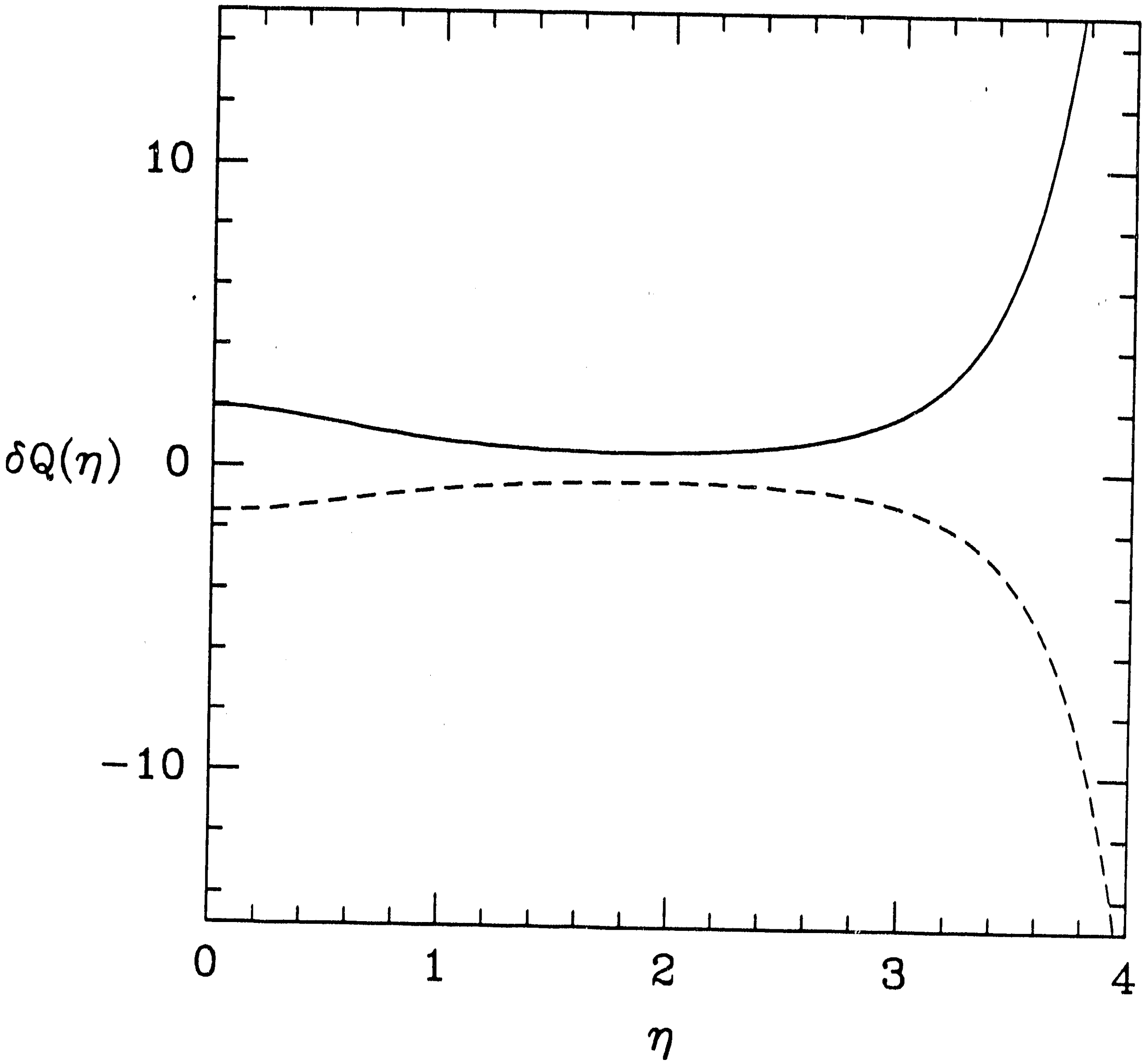

Fig. 7.

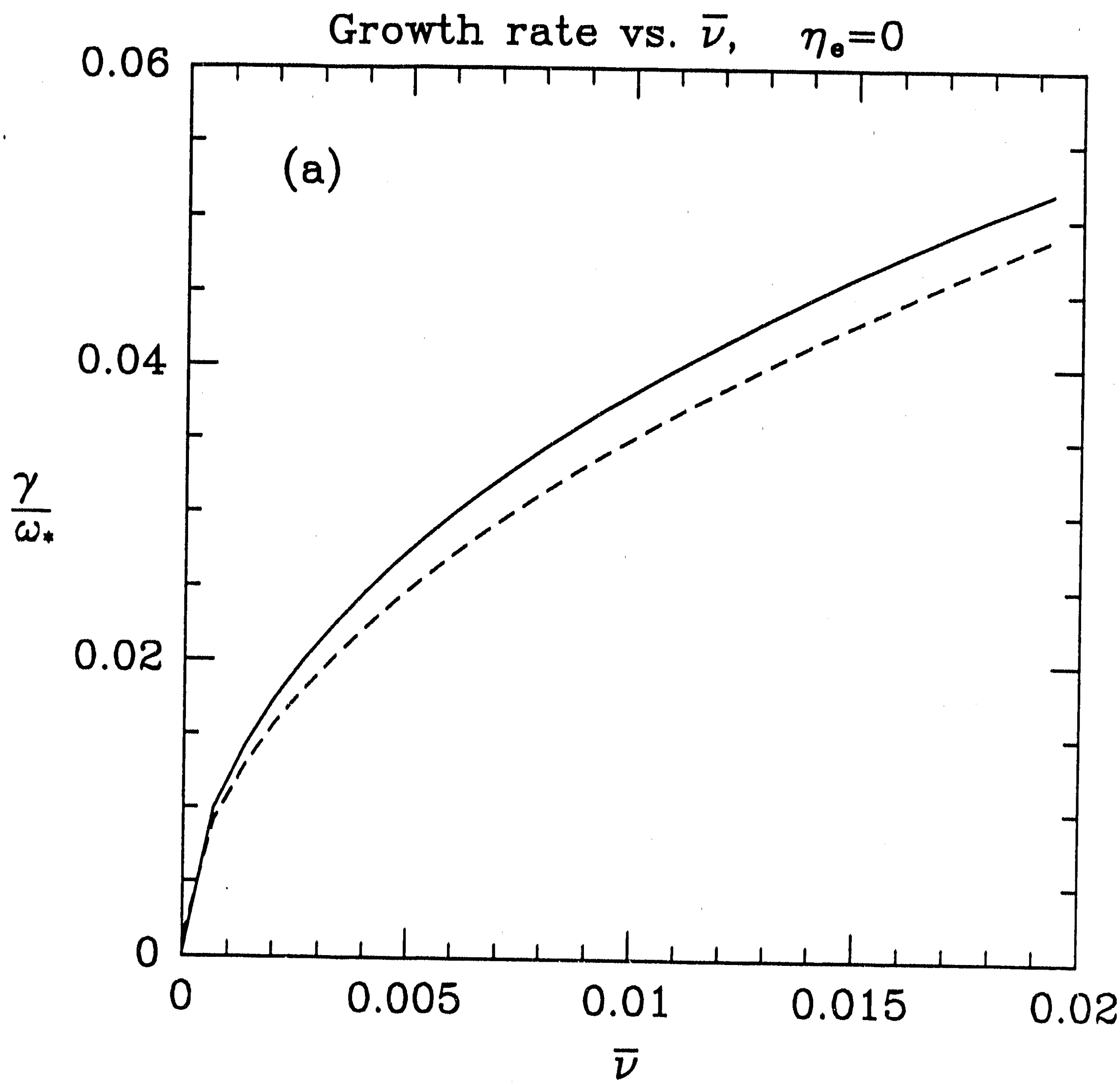
Growth rate vs. $\overline{\nu}$, η_e=0
(a)
0.06
0.04
0.02
0
$\frac{\gamma}{\omega_*}$
0
0.005
0.01
0.015
0.02
$\overline{\nu}$

Fig. 8(a).

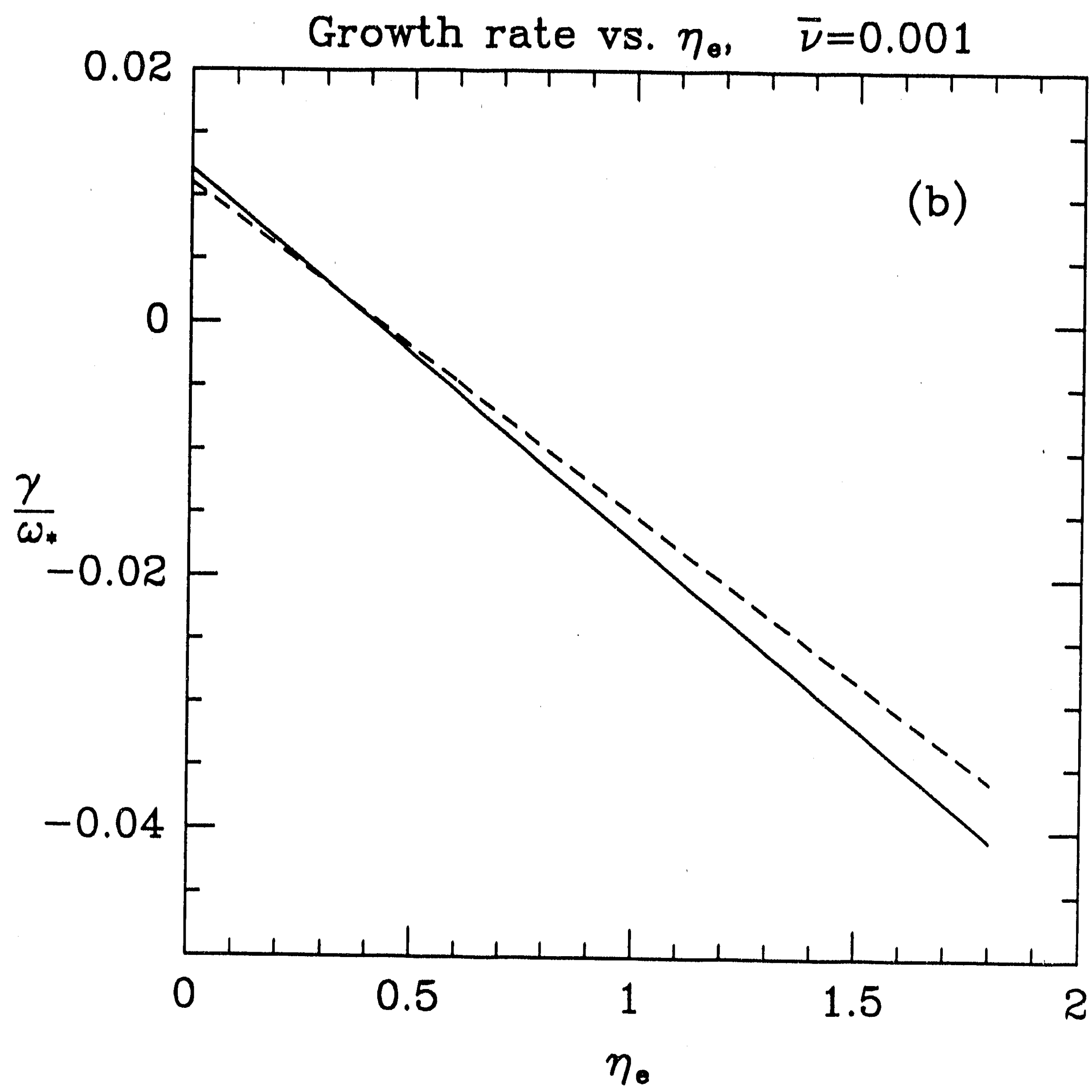

Growth rate vs. η_e, $\bar{\nu}$=0.001
0.02
0
−0.02
−0.04
$\frac{\gamma}{\omega_*}$
(b)
0
0.5
1
1.5
2
η_e

Fig. 8(b).

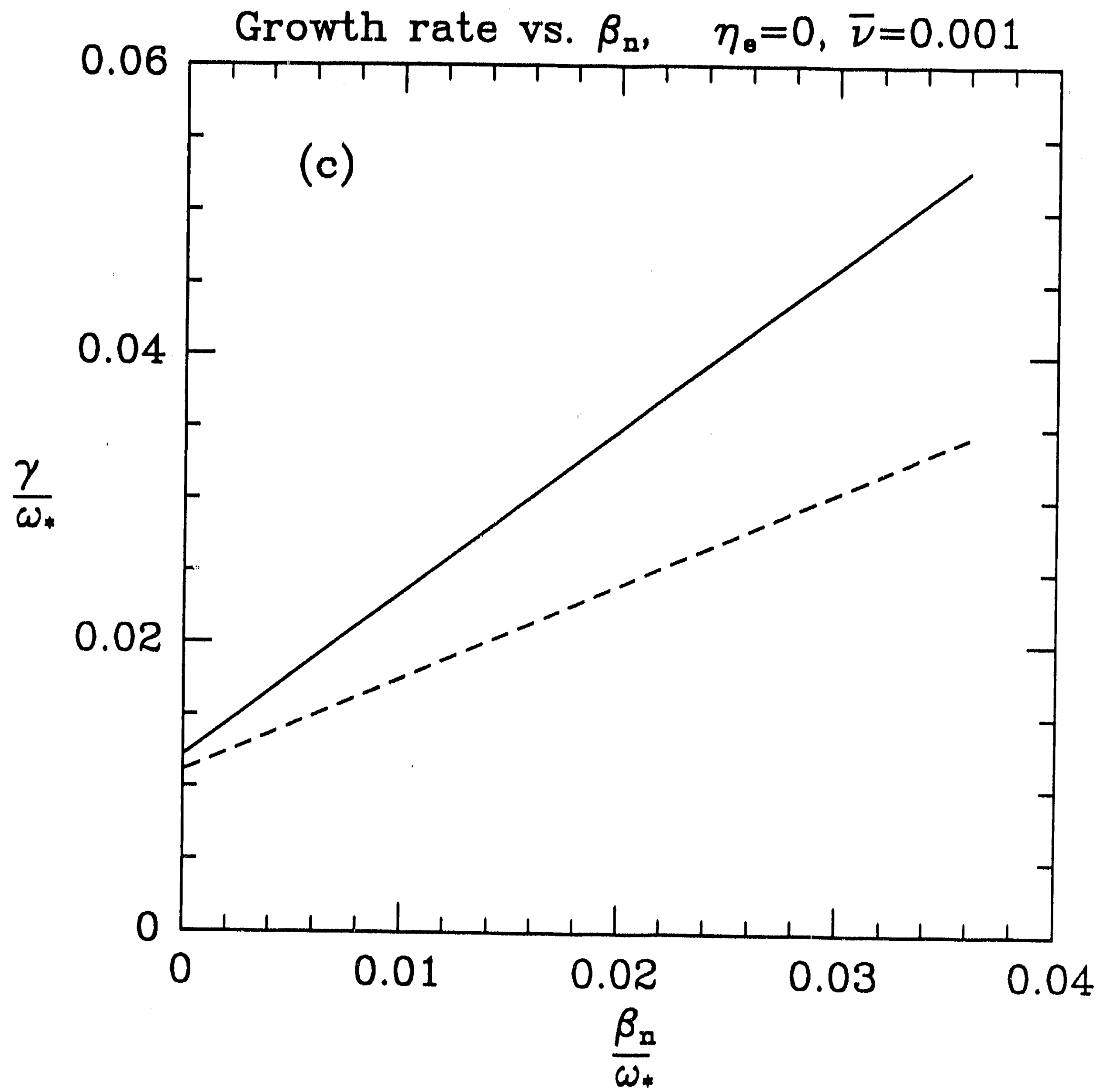

Growth rate vs. β_n, η_e=0, $\bar{\nu}$=0.001
(c)
0.06
0.04
0.02
0
$\frac{\gamma}{\omega_*}$
0
0.01
0.02
0.03
0.04
$\frac{\beta_n}{\omega_*}$

Fig. 8(c).

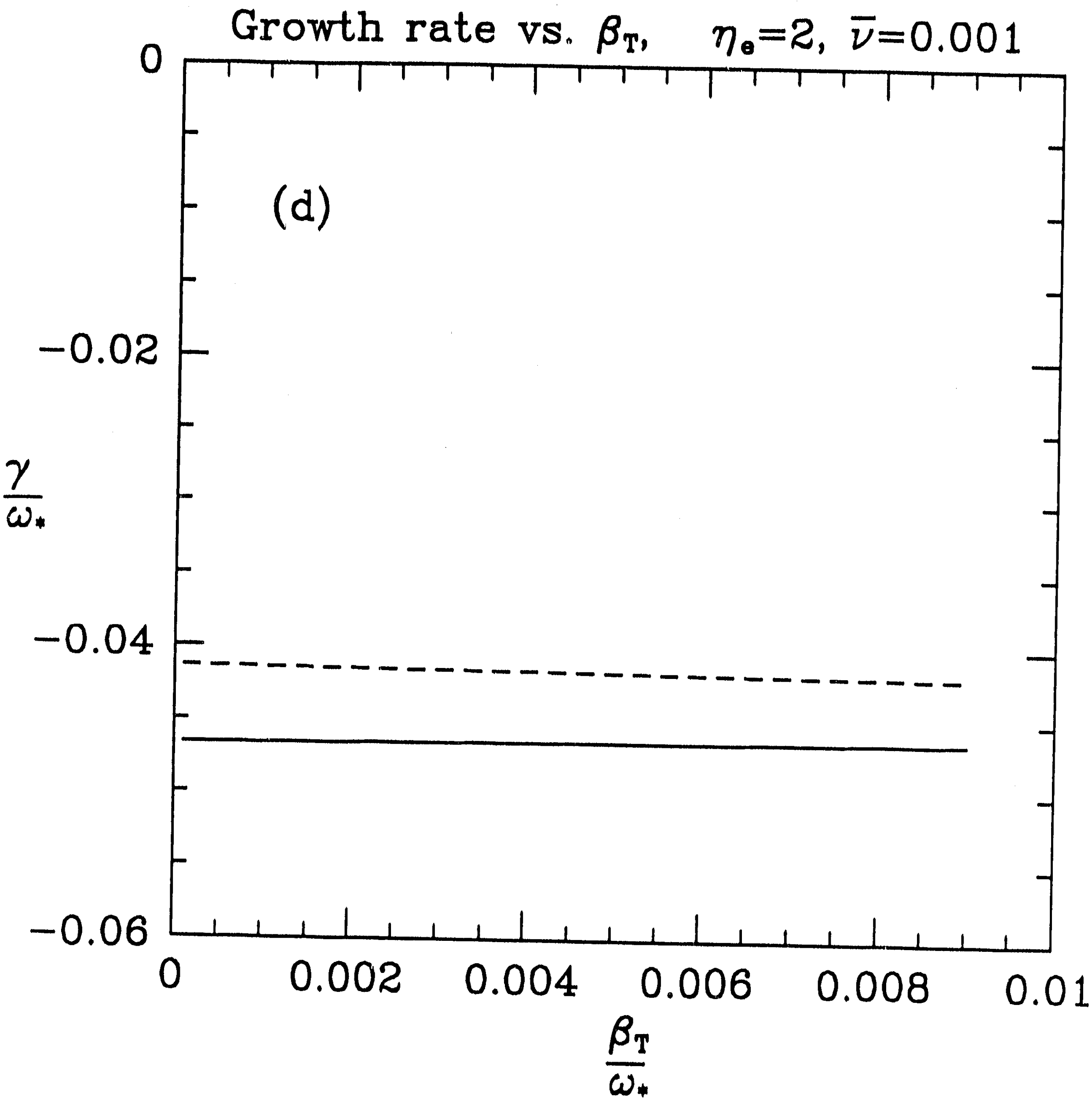
Growth rate vs. β_T, η_e=2, $\bar{\nu}$=0.001
(d)
0
−0.02
−0.04
−0.06
$\frac{\gamma}{\omega_*}$
0
0.002
0.004
0.006
0.008
0.01
$\frac{\beta_T}{\omega_*}$

Fig. 8(d).

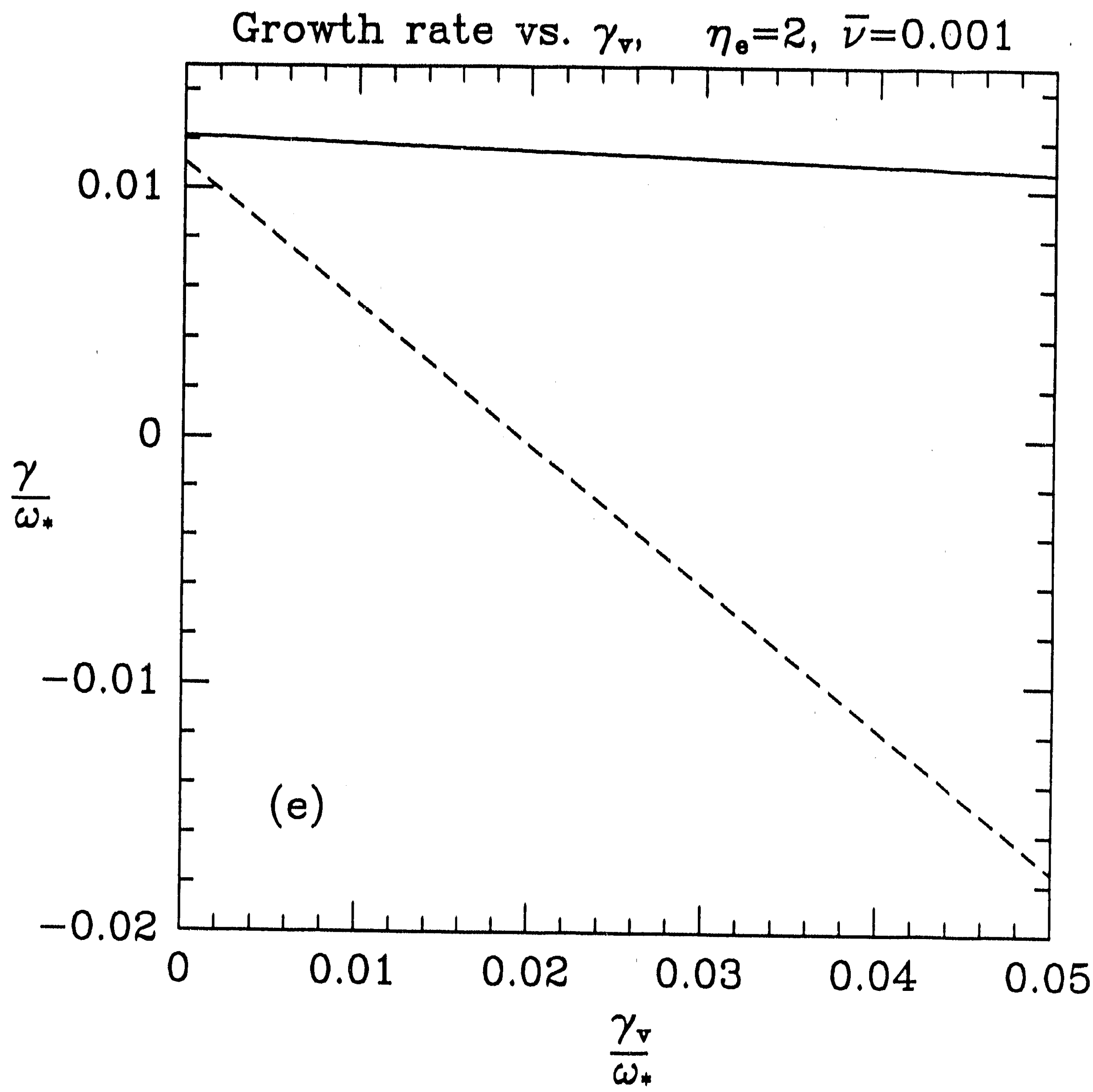

Growth rate vs. γ_v, η_e=2, $\bar{\nu}$=0.001
0.01
0
−0.01
−0.02
$\frac{\gamma}{\omega_*}$
(e)
0
0.01
0.02
0.03
0.04
0.05
$\frac{\gamma_v}{\omega_*}$

Fig. 8(e).

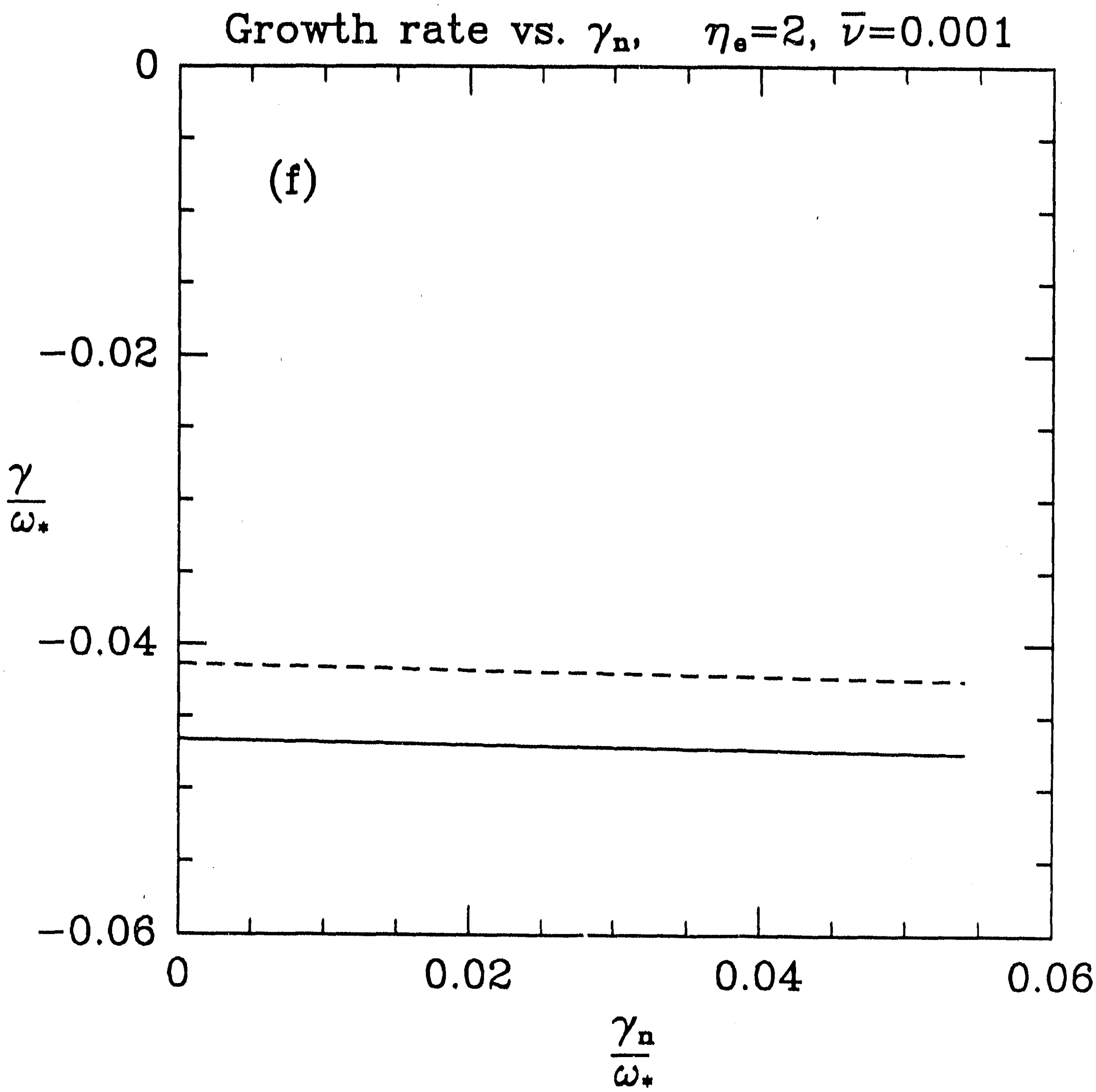
Growth rate vs. γ_n, η_e=2, $\bar{\nu}$=0.001
(f)
0
−0.02
−0.04
−0.06
$\frac{\gamma}{\omega_*}$
0
0.02
0.04
0.06
$\frac{\gamma_n}{\omega_*}$

Fig. 8(f).

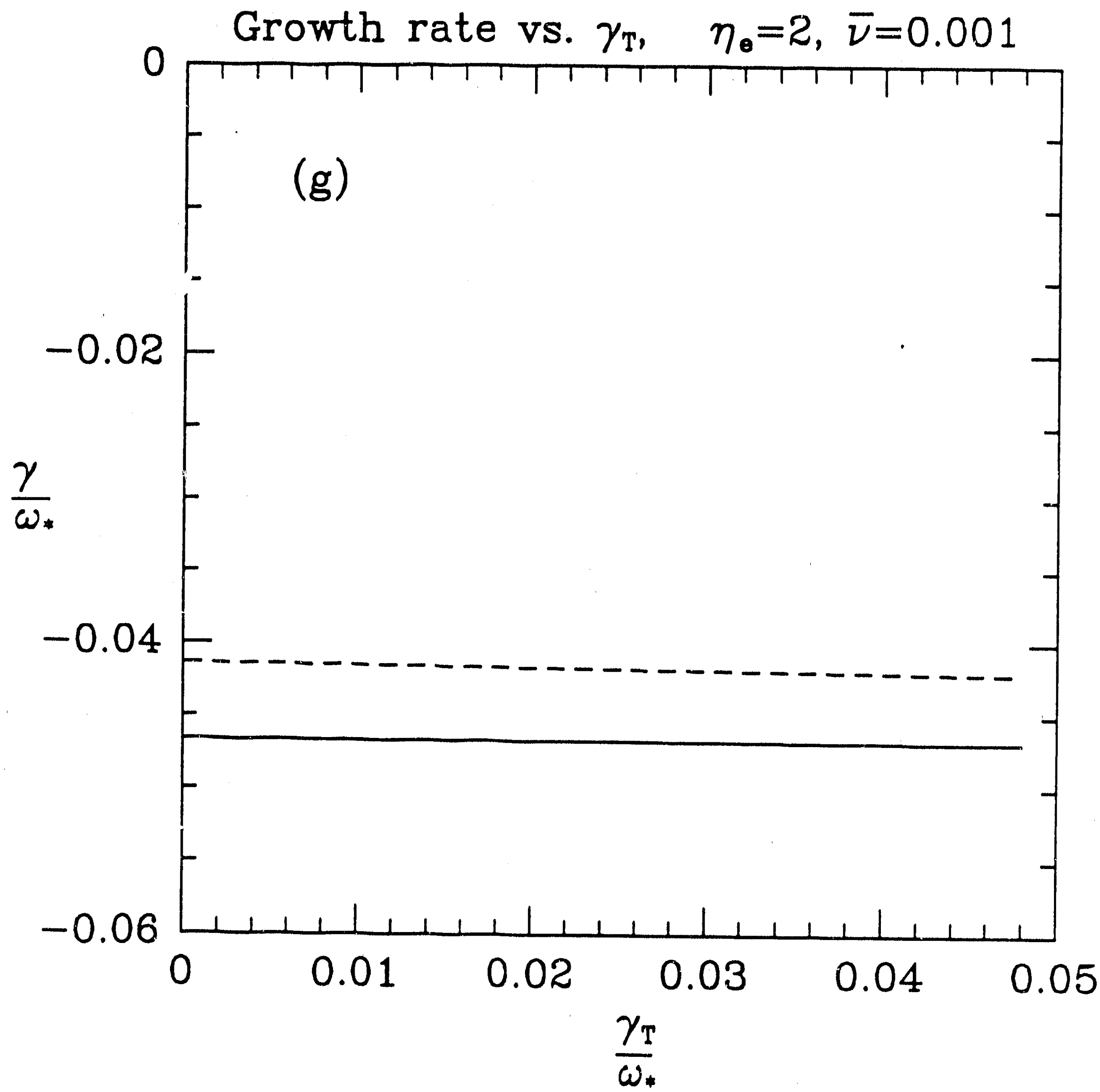

Growth rate vs. γ_T, η_e=2, $\bar{\nu}$=0.001
(g)
0
−0.02
−0.04
−0.06
$\frac{\gamma}{\omega_*}$
0
0.01
0.02
0.03
0.04
0.05
$\frac{\gamma_T}{\omega_*}$

Fig. 8(g).

EXTERNAL DISTRIBUTION IN ADDITION TO UC-420

Dr. F. Paoloni, Univ. of Wollongong, AUSTRALIA
Prof. M.H. Brennan, Univ. of Sydney, AUSTRALIA
Plasma Research Lab., Australian Nat. Univ., AUSTRALIA
Prof. I.R. Jones, Flinders Univ, AUSTRALIA
Prof. F. Cap, Inst. for Theoretical Physics, AUSTRIA
Prof. M. Heindler, Institut für Theoretische Physik, AUSTRIA
Prof. M. Goossens, Astronomisch Instituut, BELGIUM
Ecole Royale Militaire, Lab. de Phy. Plasmas, BELGIUM
Commission-European, DG. XII-Fusion Prog., BELGIUM
Prof. R. Boucique, Rijksuniversiteit Gent, BELGIUM
Dr. P.H. Sakanaka, Instituto Fisica, BRAZIL
Instituto Nacional De Pesquisas Espaciais-INPE, BRAZIL
Documents Office, Atomic Energy of Canada Ltd., CANADA
Dr. M.P. Bachynski, MPB Technologies, Inc., CANADA
Dr. H.M. Skarsgard, Univ. of Saskatchewan, CANADA
Prof. J. Teichmann, Univ. of Montreal, CANADA
Prof. S.R. Sreenivasan, Univ. of Calgary, CANADA
Prof. T.W. Johnston, INRS-Energie, CANADA
Dr. R. Bolton, Centre canadien de fusion magnétique, CANADA
Dr. C.R. James,, Univ. of Alberta, CANADA
Dr. P. Lukác, Komenského Universzita, CZECHO-SLOVAKIA
The Librarian, Culham Laboratory, ENGLAND
Library, R61, Rutherford Appleton Laboratory, ENGLAND
Mrs. S.A. Hutchinson, JET Library, ENGLAND
Dr. S.C. Sharma, Univ. of South Pacific, FIJI ISLANDS
P. Mähönen, Univ. of Helsinki, FINLAND
Prof. M.N. Bussac, Ecole Polytechnique,, FRANCE
C. Mouttet, Lab. de Physique des Milieux Ionisés, FRANCE
J. Radet, CEN/CADARACHE - Bat 506, FRANCE
Prof. E. Economou, Univ. of Crete, GREECE
Ms. C. Rinni, Univ. of Ioannina, GREECE
Dr. T. Mual, Academy Bibliographic Ser., HONG KONG
Preprint Library, Hungarian Academy of Sci., HUNGARY
Dr. B. DasGupta, Saha Inst. of Nuclear Physics, INDIA
Dr. P. Kaw, Inst. for Plasma Research, INDIA
Dr. P. Rosenau, Israel Inst. of Technology, ISRAEL
Librarian, International Center for Theo Physics, ITALY
Miss C. De Palo, Associazione EURATOM-ENEA , ITALY
Dr. G. Grosso, Istituto di Fisica del Plasma, ITALY
Prof. G. Rostangni, Istituto Gas Ionizzati Del Cnr, ITALY
Dr. H. Yamato, Toshiba Res & Devel Center, JAPAN
Prof. I. Kawakami, Hiroshima Univ., JAPAN
Prof. K. Nishikawa, Hiroshima Univ., JAPAN
Director, Japan Atomic Energy Research Inst., JAPAN
Prof. S. Itoh, Kyushu Univ., JAPAN
Research Info. Ctr., National Instit. for Fusion Science, JAPAN
Prof. S. Tanaka, Kyoto Univ., JAPAN
Library, Kyoto Univ., JAPAN
Prof. N. Inoue, Univ. of Tokyo, JAPAN
Secretary, Plasma Section, Electrotechnical Lab., JAPAN
S. Mori, Technical Advisor, JAERI, JAPAN
Dr. O. Mitarai, Kumamoto Inst. of Technology, JAPAN
J. Hyeon-Sook, Korea Atomic Energy Research Inst., KOREA
D.I. Choi, The Korea Adv. Inst. of Sci. & Tech., KOREA
Prof. B.S. Liley, Univ. of Waikato, NEW ZEALAND
Inst of Physics, Chinese Acad Sci PEOPLE'S REP. OF CHINA
Library, Inst. of Plasma Physics, PEOPLE'S REP. OF CHINA
Tsinghua Univ. Library, PEOPLE'S REPUBLIC OF CHINA
Z. Li, S.W. Inst Physics, PEOPLE'S REPUBLIC OF CHINA
Prof. J.A.C. Cabral, Instituto Superior Tecnico, PORTUGAL
Dr. O. Petrus, AL I CUZA Univ., ROMANIA
Dr. J. de Villiers, Fusion Studies, AEC, S. AFRICA
Prof. M.A. Hellberg, Univ. of Natal, S. AFRICA
Prof. D.E. Kim, Pohang Inst. of Sci. & Tech., SO. KOREA
Prof. C.I.E.M.A.T, Fusion Division Library, SPAIN
Dr. L. Stenflo, Univ. of UMEA, SWEDEN
Library, Royal Inst. of Technology, SWEDEN
Prof. H. Wilhelmson, Chalmers Univ. of Tech., SWEDEN
Centre Phys. Des Plasmas, Ecole Polytech, SWITZERLAND
Bibliotheek, Inst. Voor Plasma-Fysica, THE NETHERLANDS
Asst. Prof. Dr. S. Cakir, Middle East Tech. Univ., TURKEY
Dr. V.A. Glukhikh,Sci. Res. Inst. Electrophys.I Apparatus, USSR
Dr. D.D. Ryutov, Siberian Branch of Academy of Sci., USSR
Dr. G.A. Eliseev, I.V. Kurchatov Inst., USSR
Librarian, The Ukr.SSR Academy of Sciences, USSR
Dr. L.M. Kovrizhnykh, Inst. of General Physics, USSR
Kernforschungsanlage GmbH, Zentralbibliothek, W. GERMANY
Bibliothek, Inst. Für Plasmaforschung, W. GERMANY
Prof. K. Schindler, Ruhr-Universität Bochum, W. GERMANY
Dr. F. Wagner, (ASDEX), Max-Planck-Institut, W. GERMANY
Librarian, Max-Planck-Institut, W. GERMANY
Prof. R.K. Janev, Inst. of Physics, YUGOSLAVIA

END

DATE
FILMED
4/27/92